NTNU
Norwegian University of
Science and Technology

Spatiotemporal patterns of plant growth in a warming high Arctic: insights from dendrochronology of *Salix polaris*

Lisa Sandal

MSc in Biology
Submission date: May 2017
Supervisor: Vidar Grøtan, IBI
Co-supervisor: Mathilde Le Moullec, IBI
Brage Bremset Hansen, IBI

Norwegian University of Science and Technology
Department of Biology

Abstract

Climate change is most pronounced at high latitudes, where plant and animal populations are often strongly influenced by environmental drivers, such as climate. Theory suggests that if these environmental drivers are synchronized over large distances, this spatial synchrony should also be reflected in the population synchrony of plants and animals. In the Arctic, large-scale studies of such spatiotemporal patterns and their links to climate and climate change are rare, partly because of lack of the spatially distributed and long-term time-series required for abiotic and biotic parameters. Here, I used dendrochronological tools to analyse for climate drivers and their role in the synchronization of fluctuations in *Salix polaris* ring-width growth across large distances (n = 16 sites, maximum distance = 293 km) in high-Arctic Svalbard. While heavy winter rain-on-snow events (causing ground-ice) influenced growth negatively in some wet coastal sites, summer temperature had an overall strongly positive effect on tree-ring growth across the archipelago. Accordingly, annual plant growth was correlated across large distances (average regional synchrony ρ= 0.23, spatial scale of synchrony= 192 km), and summer temperature explained a significant part of this spatial synchrony. Interestingly, there was a marked decline in spatial synchrony of plant growth since the late 1990s, which could be partly explained by the reduced spatial synchrony in summer temperatures occurring in parallel with the overall warming trend. The results from this study, which is the first to demonstrate the role of climate in synchronizing Arctic plant growth over large distances, have potentially large implications for our understanding of how climate shapes ecosystem productivity in time and space, thereby improving our ability to predict the broader ecological impacts of climate change.

Sammendrag

Ved høye breddegrader er plante- og dyrepopulasjoner ofte sterkt påvirket av svingninger i miljøet, og det er her klimaendringene er sterkest. Klima og miljøsvingninger er ofte synkronisert over store avstander, og ifølge teorien kan denne romlige synkronien også reflekteres i fluktuasjoner i plante- og dyrepopulasjoner. Studier av slike mønstre i tid og rom, og deres koblinger til klima og klimaendringer, er sjeldne i Arktis. Dette er delvis på grunn av mangel på lange nok tidsserier med tilstrekkelig romlig fordeling for både abiotiske og biotiske parametere. I dette studiet brukte jeg dendrokronologiske verktøy for å analysere hvordan miljøsvingninger påvirker synkroniseringen av fluktuasjoner i årringvekst hos polarvier *Salix polaris* over store avstander (n = 16 lokaliteter, maksimal avstand = 293 km) på Svalbard. Mens mye vinterregn (som blir til is på bakken) påvirket planteveksten negativt i noen våte kystnære lokaliteter, hadde sommertemperaturen en generell sterk positiv effekt på årringveksten over hele Svalbard. Planteveksten var synkronisert over store avstander (gjennomsnittlig regional synkronisering ρ = 0.23, romlig skala av synkronisering= 192 km), og sommertemperatur forklarte en signifikant andel av denne romlige synkronien. Romlig synkronitet i plantevekst avtok fra slutten av 1990-tallet, noe som delvis kunne forklares ved redusert synkroni i sommertemperatur under en periode med generell oppvarming. Resultatene fra dette studiet, som er det første som viser klimaets rolle i synkronisering av arktisk plantevekst over store avstander, har potensielt stor betydning for vår forståelse av hvordan klima påvirker arktiske økosystemers dynamikk i tid og rom.

Table of Contents

Introduction 4
Methods 7
Study area and species 7
Sample collection 7
Laboratory preparation and growth measurement 7
Cross-dating and chronology development 9
Climate variables 10
Statistics 11
Chronology standardization 11
Local analysis 12
Regional analysis 12
Synchrony analysis 13
Results 15
Chronologies 15
Local analysis 15
Regional analysis 15
Synchrony analysis 16
Discussion 17
Acknowledgements 21
References 22
Tables and Figures 28
Appendix 39
Weather station data 39
Chronologies 40
Local analysis 43
Regional analysis 44
Synchrony analysis 45

Introduction

The Earth's climate is changing, and nowhere else is global warming more pronounced than in the Arctic (IPPC 2014, Nordli et al. 2014). Plant and animal populations at high latitudes are often strongly influenced by environmental variation (Bjørnstad and Stenseth 1995, Sæther et al. 2003), making Arctic species particularly vulnerable to the observed rapid climate change (Ims and Ehrich 2013). Environmental fluctuations (i.e. weather) are often correlated over large distances (Koenig 1999), and Moran (1953) suggested that populations may be synchronized over similarly large spatial scales if they are strongly influenced by these environmental variables (the "Moran effect"). Quantifying spatial patterns of temporal co-fluctuations in for example population sizes (i.e. spatial population synchrony) is therefore of fundamental importance in predictions of large-scale ecosystem impacts of climate and climate change (Post et al. 2009, Sheppard et al. 2015).

Spatial population synchrony can be observed over large distances in a wide range of taxa (Bjørnstad et al. 1999, Koenig 1999, Liebhold et al. 2004, Sæther et al. 2007). The Moran effect is only one of three main groups of mechanisms proposed to explain such synchronous responses among populations (Moran 1953, Royama 1992, Lande et al. 1999, Engen et al. 2002, Engen et al. 2005, Engen and Sæther 2005, Sæther et al. 2007). Dispersal can also cause spatially correlated fluctuations in abundance by linking sub-populations together (Engen et al. 2002, Lande et al. 1999). Also, interactions with species at the same or different trophic levels may cause between-species synchrony, either through dependency on synchronized populations at lower or higher trophic levels (Liebhold et al. 2004), or through nomadic predators (or herbivores) focusing on prey hotspots (Ydenberg 1987, Ims and Andreassen 2000).

There are several simplifying assumptions underlying Moran's original theorem (e.g. no migration between populations, equal (log-)linear density regulation in all populations and homogeneity in population responses to environmental variables) (Moran 1953, Royama 1992, Engen et al. 2005), so that in reality, the spatial scale of synchrony among populations is generally much lower than that of the environmental drivers (Stenseth 1999, Sæther et al. 2003, Sæther et al. 2007). Nevertheless, the Moran effect is often regarded as the mechanism contributing the most to the large spatial scales at which population synchrony can often be observed (Massie et al. 2015). Accordingly, the Moran effect has been demonstrated in several vertebrates, such as the Soay sheep (*Ovies aries*) on islands off Scotland (Grenfell et al. 1998), roe deer (*Capreolus capreolus*) in Boreal ecosystems (Grøtan et al. 2005), and passerine birds in Europe (Sæther et al. 2007). On the contrary, relatively few studies have examined the role of the Moran effect in plant species (but see e.g. Post 2003, Läänelaid et al. 2012, Rosenstock et al. 2011, Koenig and Knops 2013). This is surprising, given the general and strong direct

influence of climatic drivers such as temperature on vital rates in many plant species (Barbour et al. 1980, Woodward 1987) as well as the role of primary production in shaping the dynamics of many bottom-up systems, such as the Arctic tundra (Power 1992, Ims and Fuglei 2005, Oksanen et al. 2008, Ims et al. 2013).

In the light of recent climate change, understanding the level of spatial synchrony and the climatic contribution to it is more important than ever, because the Moran effect implies that independent biological populations over large areas might respond similarly to changing climatic conditions (Post and Forchhammer 2002). High synchrony in population fluctuations over large distances is likely to increase the vulnerability to extinction (Ranta et al. 1995, Heino et al. 1997, Engen et al. 2002, Post et al. 2009). This is particularly relevant if the level of spatial synchrony changes over time (e.g. Post and Forchhammer 2002, Läänelaid et al. 2012, Sheppard et al. 2015). However, quantifying the relative role of different mechanisms (i.e. Moran effect, dispersal, trophic interactions) causing synchrony is difficult in many species, since these are not mutually exclusive and may affect populations simultaneously in various combinations (Liebhold et al. 2004, Estay et al. 2011). It may hence be easier to partition out the climatic contribution to synchrony in spatially separated plant populations, where the challenges related to dispersal and movement are negligible.

Svalbard, a Norwegian archipelago of the high Arctic, is a relatively well-studied ecosystem with a simple, bottom-up controlled terrestrial food web (Ims et al. 2013). The major role of primary production in this system calls for a better understanding of spatiotemporal patterns in plant growth, especially since the annual fluctuations of the resident vertebrate community has been shown to be synchronized across species through climate events that limit herbivores' access to forage plants (Hansen et al. 2013). Both summer temperature (strongly influencing primary production in the Arctic, e.g. Henry and Molau 1997, Aanes et al. 2002, Buchwal et al. 2013, van der Wal and Stien 2014) and, in particular, winter rain-on-snow (ROS) events (causing ice-locked herbivore pastures) contribute to the observed cross-species synchrony. However, the scale at which these climate drivers of community-level dynamics act on the spatial synchrony of species abundances is not well known (but see Aanes et al. 2003). On Svalbard, climatic conditions differ from the west coast, which is strongly influenced by the warm Gulf Stream, to the east coast, which is under more influence from the Arctic Ocean and the surrounding Sea Ice (Sakshaug et al. 2009, Johansen et al. 2012), and such geographical differences may cause differential growth responses to regional-level climatic variation, potentially also causing heterogeneity in the temporal ecosystem dynamics.

Studying spatiotemporal dynamics requires long and spatialy distributed time-series, which are extremely difficult to obtain in the Arctic. Woody plant species contain valuable, long-term growth records, that, especially in bottom-up controlled systems such as high-Arctic Svalbard, can provide

important insight into ecosystem dynamics. Dendrochronological tools have only recently been developed to be applicable to dwarf-shrubs, allowing us to obtain long-term growth-records also from biomes above the tree line (Woodcock and Bradley 1994, Schweingruber and Poschlod 2005, Myers-Smith et al. 2015b). Applying dendrochronology, i.e. the dating of annual growth rings, to dwarf-shrubs has previously proven to be a useful tool for instance for investigating past climate, studying the relationship between growth and climate change, reconstructing glacial history and dating landslides (Gers et al. 2001, Schmidt et al. 2006, Owczarek 2010, Buras et al. 2012, Rayback et al. 2012a, Myers-Smith et al. 2015a).

In Svalbard, there is one species that meets the requirements to undertake dendrochronology at large spatiotemporal scales: the polar willow *Salix polaris* (Wahlenberg). The polar willow is a long-lived, widespread and abundant shrub in Svalbard (Rønning 1996), constituting a major part of the primary production (van der Wal and Stien 2014) and making it possible to sample across the whole archipelago. The dwarf-shrub *Cassiope tetragona* has also shown potential for dendrochronological studies at high latitudes (Rayback and Henry 2005, Rayback et al. 2012a), but the species is only found in warmer valleys of Svalbard (Rønning 1996) and is thus unsuitable for this study. In addition, ring-width indices of *S. polaris* have been found to accurately reflect its fluctuations in past aboveground biomass production, as well as the general community primary production (Le Moullec et al. in prep.), making dendrochronology applied to this species a valuable tool to improve our understanding of spatiotemporal variation in ecosystem dynamics in a rapidly changing high Arctic. While dendrochronological tools have been used on *S. polaris* at three sites in Svalbard, i.e. Hornsund, Petuniabukta and Semmeldalen (Owczarek 2010, Buchwal et al. 2013, Le Moullec et al. in prep.), it has never before been attempted to estimate the spatial scale of synchrony in primary production across large distances in the Arctic. Many sites are difficult to access, and large areas (e.g. the eastern parts) are therefore largely unstudied in a tundra ecosystem context, possibly causing bias in interpretation of ecological climate change effects.

Thus, in this study, I reconstruct and compare growth curves of *S. polaris* collected across Svalbard in order to answer the following research questions: Q1: What are the main climatic variables influencing tree-ring growth, an annual plant growth proxy, and are there differential responses to these among sites? Q2: To what extent is shrub growth synchronized across Svalbard, and what is the climatic contribution to this synchrony and Q3: Does the level of synchrony change over time, and if so, can this be linked to climate change?

Methods

Study area and species

Around 60% of the land area of Svalbard (ca. 74–81°N, 10–35°E) is covered by glaciers, while only ca. 13% is vegetated (Hisdal 1985, Johansen et al. 2012). The archipelago has a relatively mild climate for its northern location, and shows high inter-annual variability in air temperature (Johansen et al. 2012, Hansen et al. 2014, Nordli et al. 2014). An overview of the spatial gradients in modelled temperature and precipitation across our sample sites is presented in Table 1 using ERA-Interim climate reanalysis data downscaled to 1 km horizontal resolution as provided by Østby et al. (2017).

S. polaris is a prostrate species with often only shoot tips, leaves and reproductive structures visible above-ground (Rønning 1996) that reproduces both sexually and clonally through rhizomes (Gornall et al. 2011). The branches emerge from the root collar complex, i.e. the oldest part of the plant, which is situated on top of the central root. The below-ground structure usually consists of one main taproot which can extend several decimetres into the ground, and several thin secondary roots (Buchwal et al. 2013). *S. polaris* is an important food resource for both the resident herbivores, i.e. Svalbard reindeer (*Rangifer tarandus platyrhynchus*) and Svalbard rock ptarmigan (*Lagopus muta hyperborea)*, as well as for migratory geese (*Branta* sp*.)* (van der Wal et al. 2000, Bjørkvoll et al. 2009).

Sample collection

Samples of *S. polaris* were collected in summer 2015 from seven sites on Svalbard, covering central parts as well as the eastern, western and southern coast (Figure 1). Chronologies from Semmeldalen (9 independent sub-sites) were developed in a separate study by Le Moullec et al. (in prep.). In addition, data from Petuniabukta was collected in 2010, see Buchwal et al. (2013).

In accordance with Myers-Smith et al. (2015b) large individuals without visible injuries were selectively sampled for the construction of the growth chronologies. The most well-developed individuals were usually found growing in isolation and forming dense cushions on pioneer vegetation terrain such as raised beeches. Individuals were selected with a minimum distance of 10 m to avoid sampling genetically identical organisms. All samples from a location were collected within a radius of 50-80 m, with similar terrain, exposure and slope. At Sørkapp, shrubs were collected from two similar subsites five km apart. In total, chronologies were developed from 67 plants from 16 independently cross-dated sites, with a minimum of five plants (i.e. minimum 92 radial measurements) per site (Table 1).

Laboratory preparation and growth measurement

Cross-dating, i.e. aligning each annual growth measurement to the correct calendar year, is the most essential step in reconstructing correct chronologies of past growth (Buchwal et al. 2013, Myers-Smith

et al. 2015b). Arctic shrubs are adapted to tolerate high variability in their physical environment (Crawford 1997), and growth may consequentially be allocated differentially to above- and belowground parts (Buchwal et al. 2013, Myers-Smith et al. 2015b) in response to local stressors affecting the individual, such as grazing and trampling, competition, frost heave in soils, flooding after thaw etc. (Billings 1987, Jonasson and Callaghan 1992, Speed et al. 2011). Consequently, rings may be missing in some parts of the plant but detectable in others (locally missing rings [LMRs]), or even absent in the whole plant (missing rings [MRs]) (Polunin 1955, Buchwal et al. 2013). Such MRs can be detected in other plants from the same location. In addition, dwarf-shrubs often exhibit eccentric growth, and rings may be accordingly wider or more narrow in some parts of a cross-section, causing partially missing rings (PMRs) where two or more rings are no longer clearly separable from each other (Buras and Wilmking 2014, Myers-Smith et al. 2015b).

To succeed in this cross-dating task, serial sectioning was applied (Buchwal 2014). Serial sectioning involves sampling the individual plant at multiple points along roots and branches (Kolishchuk 1990, Woodcock and Bradley 1994, Myers-Smith et al. 2015b), and has been applied successfully in a number of studies (e.g. Bär et al. 2006, 2007, Büntgen and Schweingruber 2010, Blok et al. 2011, Hallinger and Wilmking 2011, Buchwal et al. 2013). Five to six thin cross-sections from each individual were made, depending on the degree of irregularity of the plant, including above- and belowground parts of the plant. Following Myers-Smith et al. (2015b), at least one cross-section always originated from the root collar. In addition, two- three more cross-sections were cut from the central taproot, and/or relevant old side roots, as well as two cross sections from branches (except in a few cases where only one high-quality branch cross-section could be obtained). Thin cross-sections (15-20 µm) of the specimens were cut at ca. 2-5 cm distance from each other using a GSL1 microtome (Gärtner et al. 2014, Tardif and Conciatori 2015). In order to make tree-rings clearly distinguishable, a 2:1 solution of aqueous Astra Blue (1g/1000 ml) and aqueous Safranin O Dye (1g/1000 ml), was used to stain lignified structures pink and the cellulose in the unlignified cells of the annual rings blue (Vazquez-Cooz and Meyer 2002). During staining, cross-sections were handled using soft brushes and manually de-sharpened glass Pasteur pipettes with rounded tips, to avoid injuring the tissue. To remove any impurities, the cross-sections were washed by maintaining an energetic flow of distilled water through the pipette, while gently holding the sample in place with the rounded tip. A drop of staining solution was placed on the cross-sections with a staining-time of 4 minutes, and then washed and dehydrated in a series of ethanol-treatments with increasing purity (70%, 95% and 100%). Each treatment consisted of rinsing the cross-sections for 5 minutes using the pipette as described above. The cross-sections were permanently fixed on a microscope slide by applying Canada Balsam and letting the resin harden in an

oven at 60 °C for at least 12 hours (Schweingruber and Poschlod 2005, Buchwal et al. 2013, Myers-Smith et al. 2015b, Tardif and Conciatori 2015).

Microscope slides were cleared of any excess Canada Balsam by gently cleaning with 95% ethanol, and then digitalized at a magnification of 10x using a Nikon Eclipse E800 light microscope with a Nikon Ds-Ri1 camera. The software NIS-Elements (Nikon) was used for capturing the pictures. This procedure resulted in ca. 15-150 pictures per cross-section, depending on diameter, and these were merged using the panoramic image stitching software AutoStitch (Brown 2015). Due to the selective sampling of large and regular individuals, my cross-sections only show mild eccentricity. Buras and Wilmking (2014), suggest a minimum of two radial measurements for such cross-sections, but to reduce dating errors and to accurately account for the shape of each cross-section, four radial measurements were done. The four radii were defined by first dividing each cross-section image into four quarters, excluding areas with injuries or staining impurities that would compromise the reliability of the measurements. Mostly, the whole area could be considered for measurement. Within each of the four quarters, one radius was selected randomly. Using the radius as starting point, tree-ring width (TRW) in µm was measured in ImageJ (Schindelin et al. 2015) as the perpendicular line between ring boundaries. Measurements where done from the cambium towards the center of the cross-section, stopping at the youngest clearly defined ring. For standardization purposes, the total length of the radii was measured, and approximate number of remaining years to the pith not measured was recorded.

Cross-dating and chronology development

Myers-Smith et al. (2015a) describe cross-dating as a hierarchical process with cross-dating 1) between radial measurements of a cross-section, 2) between all the cross-sections of one plant to obtain a correct chronology of each individual, and 3) between plants. In addition, as suggested by Wils et al. (2009), it was necessary to move back and forth between these different levels of cross-dating.

1) Cross-dating of radial measurements within cross-sections: One approach to cross-dating is the matching of measurements based on positive pointer years (Schweingruber et al. 1990), i.e. well developed continuous wide rings. Such reference rings were colour-marked to ensure that each of the four radial measurements within a cross-section was aligned correctly. To obtain a correctly dated chronology, it is extremely important that PMRs are only included in the time-series if clearly recognizable as such. PMRs are sometimes noticeable only as a small area of double ring-boundaries, and can be difficult to detect/ distinguish from injuries. To prevent introducing erroneous rings, all indications of PMRs were checked with a Nikon Eclipse E800 light microscope. Remaining uncertainties were kept track of and resolved at a higher level of cross-dating.

2) Cross-dating between cross-sections within individuals: Printed pictures of cross-sections within a shrub were cut in half and compared pair by pair. Reference rings were clearly visible throughout the whole shrub, making it possible to align the chronologies obtained for each cross-section correctly. For an illustration of this procedure, see Appendix, Figure S1. In addition, the digital pictures were viewed on a computer screen for checking critical structures in detail. Detected MRs were introduced in the mean chronology of the cross-section and marked with a specific colour code. From these, mean chronologies for each individual shrub were obtained.

3) Cross-dating between plant chronologies within a site: all individual chronologies from one site where viewed together in one graph. Reference rings were identifiable as characteristically large TRWs in the chronologies. If the chronology of one plant showed an obvious one-year shift in its time-series pattern compared to another plant, a missing year was introduced in all cross-section chronologies of this plant, and marked with a specific colour code. Consecutive MRs at the plant level were rare, but occurred. Introduced MRs were often matching with comments marked at step 1), or could be detected when re-checking the cross-sections with the microscope. Nonetheless, some MRs had, by definition, no signs of evidence. Mean chronologies were obtained using all individual chronologies per site, and are presented only for the time-spans covered by a minimum sample depth of 10 cross-sections (Figure S2). No cross-dating was conducted between sites except for the introduction of the year of collection (2015) in Diskobukta. Shrubs from Diskobukta originate from a location at ca. 100 masl. and where collected in early summer (10th of July), thus shortly after the snowmelt. No sign of tree-ring formation for the year of collection was yet detectable (Rathgeber et al. 2016).

The package dplR (Bunn 2008) for R (R Core Team 2016) was used to calculate the average correlation between cross-section chronologies from the same shrub (rbar.wt) and the average inter-series correlation between chronologies from different shrubs within a site (rbar.bt), as well as the Expressed Population Signal (EPS) (Table 1). EPS is an evaluation of how closely the observed mean chronology (based on the finite sample collection) represents a hypothetical mean based on an infinitive number of cross-sections (Wigley et al. 1984, Cook and Pederson 2011).

Climate variables

A set of climate variables thought to influence *S. polaris* growth on Svalbard were selected *a priori* (See Table S1 for detailed information on weather station data). In addition to the strong impact of summer temperature on plant growth in the Arctic (Aanes et al. 2002, Buchwal et al. 2013, van der Wal and Stien 2014, Myers-Smith et al. 2015a), Wahren et al. (2005) suggest that summer precipitation may promote growth by deepening the active layer of the soil. Amount and type of winter precipitation also affects shrub growth in the Arctic: snow-cover may be beneficial to plants in terms of increased

insulation (Hallinger et al. 2010), but may shorten the growing season by delaying melt-out (Semenchuk et al. 2013). Spring onset is also temperature-dependent, and may influence plant performance at high latitudes (Aerts et al. 2006, Wipf et al. 2009). Precipitation falling as rain during winter (rain-on-snow (ROS) events) may lead to ground-ice formation (Hansen et al. 2014) that can possibly induce cell-death by reducing soil oxygen levels (Preece and Phoenix 2014, Milner et al. 2016). Compensatory growth in surviving parts of the plant following ROS-events have been reported in *Cassiope tetragona* (Milner et al. 2016).

Hence, monthly average temperature (°C) and total precipitation (mm) during summer, as well as total precipitation (mm) falling as snow (temperature <1 °C) or rain (temperature ≥1 °C) during winter (November-April) and spring onset were considered important climatic covariates. ROS was ln-transformed after adding one unit. Summer was defined here as July, the month most likely to reflect the peak growing season across the whole archipelago, and spring onset as the Julian day when the smoothed daily temperature (over 10 days) crossed 0 °C (Hansen et al. unpubl.).

Statistics

Chronology standardization

A major challenge in dendrochronology is to successfully disentangle the effect of climatic influences from other factors that simultaneously affect growth. For example, trees often exhibit increased growth in their developmental phase compared to in their adult phase (Briffa and Melvin 2011, Bowman et al. 2013). Standardizing the chronologies by the growth trend found when aligning chronologies by cambial age (regional curve standardization [RCS]) attempts to account for such age-related trends (see for example Biondi and Qeadan (2008)). Aligning my chronologies by age (after setting number of years not measured as an offset) did not reveal any age-related trend (Figure S3), and hence RCS was not applied. In addition, stem and root diameter increases as trees become older, so that annual ring-width decreases correspondingly (Biondi and Qeadan 2008, Buras and Wilmking 2014). The geometric trend was accounted for by transforming TRW-measurements to basal area increments (BAI) (LeBlanc 1990, Visser 1995, Biondi and Qeadan 2008). This approach assumes circular cross-sections, which is not always the case for shrubs (Buras and Wilmking, 2014). However, a study by Buras and Wilmking (2014) concluded that moderate eccentricity is reasonably well- accounted for by averaging four radial measurements, as was done in this study. The chronologies for Petuniabukta were published as non- standardized TRW measurements (Buchwal et al, 2013). Chronologies from Semmeldalen are BAI-transformed and, since their study-design did not allow for selective sampling, a juvenile effect was detected and corrected for using RCS (Le Moullec et al. in prep.).

These differences in standardization methods make direct comparison difficult. To bring growth measurements into comparable scales, chronologies were mean standardized at plant level. To minimize the risk of detecting spurious correlations with climatic variables due to common trends (possibly with no causal links), linear detrending was applied to the chronologies, as well as to any covariates to which these were compared. More specifically, all individual chronologies and climate variables are detrended for the maximum overlapping time-span at each site. Any detected correlations in co-fluctuations, rather than in trends, also suggest a causal relationship with higher certainty. These standardization steps resulted in comparable, dimensionless ring-width indices (RWI).

Local analysis

I first analysed the effects of local climate on *S. polaris* growth for the sample sites where long-term weather station data was available close by (max. ca. 30 km distance). I fitted linear mixed effect models (LMMs) with the (detrended) candidate climatic variables, as well as growth at time *t*-1 (taking into account a possible first-order autocorrelation) as fixed effects. All climatic variables in the models were correlated less than 0.5 at all sites. Year was included as random effect on the intercept to account for dependency among plants because of environmental conditions not captured by the fixed effects. Plants within each site are non-independent (due to shared environment and through cross-dating), but since growth data is detrended (i.e. 0 mean for all plants), the effect of plant on the intercept was 0, and was therefore not included as random intercept effect. No signs of a substantial random slope effect of the climatic variables on plant growth were found (analysis not presented).

Candidate models were compared using the Akaike Information Criterion corrected for low sample size (AICc) (Burnham and Anderson 2002) obtained from models fitted using maximum likelihood (ML), facilitated by the "dredge"-function from the R package MuMIn (Bartoń 2013). Estimates were subsequently obtained from the most parsimonious models, fitted with restricted maximum likelihood (REML) (Table 2). The underlying model assumptions were checked for the best models using diagnostic plots. The highest-ranking models (ΔAICc<2) are given in Table S2.

The selected models at each site differed in structure of fixed effects, and hence to visually compare the effect of a given climate variable on growth between sites, the influence of all other fixed effects specific to each model (and the influence of the random effect, common in all models) on growth, needed to be accounted for. I used the "remef"- function from the R package remef (Hohenstein and Kliegl 2015) to obtain partial residuals in growth, and plot them against the covariate of interest.

Regional analysis

As weather station data (Table S1) of adequate time-span, resolution and proximity to sample sites was not available in all cases, I used the available data to estimate the climate variables for Svalbard in

general at any given year, using a LMM with year as fixed effect and weather station as random effect on intercept.

To test for differential growth responses among sites, a LMM was fitted, where the fixed effects were site as interaction term with the detrended estimated climate variables, as well as with growth at time *t*-1. Year was included as random effect on the intercept. Again, note that the detrending removed differences among plants, and hence among site means, so that neither would be able to explain any random variation in intercept. Model selection (see Table S2) was performed using the same approach as in the local analysis, but to avoid overparameterization, a maximum of six terms (i.e. independent variable names), excluding intercept, were allowed in the candidate models (option "m.lim" in the "dredge"-function).

In addition, to identify potential synchronizing variables, I fitted a LMM with the same structure as the regional model, but where site was not included as a fixed effect (see Table S2 for model selection). This model is later referred to as the "Svalbard" model. The growth estimates obtained from this model represented the general Svalbard *S. polaris* chronology.

I also investigated the potential of summer and winter Arctic Oscillation (AO) indices, a regional climate proxy (Aanes et al. 2002, Stenseth et al. 2003), and fluctuations in Sea Ice extent in the Barents Sea to reflect the climate variables influencing plant growth. To avoid overparameterization, and because some of these proxies would reflect weather covered by the climate variables (e.g. summer AO and summer climate), the effects of these proxies were analysed separately by fitting the same models as described above.

Synchrony analysis

In the spatial analysis I compare chronologies from 16 independently cross-dated sites. Nine of these sites were located in Semmeldalen, thus making it possible to study the synchrony also at short distances. The longest time-span for which pairwise correlations were calculated was 48 years (Petuniabukta and Hornsund), and the maximum distance between sites was 292 km (Sørkapp and Ny-Ålesund).

The non-parametric correlation function for spatiotemporal data (Sncf) from the package ncf (Bjørnstad 2016) was used to explore synchrony between average RWI chronologies for all independently cross-dated sites (n=16) (i.e. pairwise correlations between chronologies) as a function of distance between them. The "Sncf"-function uses a smoothing spline to continuously model synchrony as a function of distance between sites (formulae in Bjørnstad et al. 1999) with associated 95% bootstrapped confidence envelopes (using 1000 resamples). This function also calculates the regional average synchrony, i.e. the average value of the pairwise correlations across all distances, with

associated bootstrapped 95% confidence interval. Populations were considered to be significantly synchronized if this confidence interval did not include zero (Nieminen 2015). According to Bjørnstad et al. (1999), the spatial scale of synchrony can for example be defined as the distance at which the synchrony is no longer significantly different from zero. This was interpreted to be the distance at which the lower confidence interval of the Sncf crosses zero (Eberhart-Phillips et al. 2016).

The climatic contribution to synchrony of the main climatic driver was evaluated by estimating the spatial correlation in growth when accounting for the effect of the climate variable. This was done by comparing average chronologies for each site constructed using residuals from ordinary linear models (LMs) with growth as response variable and the detrended regional estimate of the climatic variable as the predictor. The use of LMMs with year as random effect would not be appropriate in this case, as this would remove the very thing we are interested in, i.e. the remaining synchrony. To visualize the synchronizing effect of the climate variable over large distances, I estimated the Sncf for the difference between the pairwise correlations in growth (ρ) and in residual growth (ρ_{res}). To evaluate statistical significance of the climate variable's contribution to synchrony, a two-sided 95% confidence interval of the difference in bootstrapped replicates of average regional synchrony (n=1000) before and after accounting for the climate variable were calculated using the 2.5th and 97.5th percentiles.

Lastly, to identify a potential temporal trend in synchrony, the annual average regional synchrony was estimated. After z-standardizing the growth data, we can assume a multivariate normal distribution at each year *t*,

$$\psi_{\boldsymbol{t}} \sim \mathrm{MVN}(0, \Sigma) \quad (1)$$

where Σ is a covariance matrix (which, for z-standardized data, equals the correlation matrix) with diagonal elements equal to 1 and off-diagonal elements equal to the average regional correlation. The average regional synchrony for each year can be estimated as the value (between -1 and 1) of these off-diagonal elements that maximizes the likelihood of the observed data. The yearly average regional synchrony was estimated for the time-span including the maximum amount of sites (1989-2014) (but note that the chronologies for Petuniabukta stop in 2010).

All statistical analyses were performed in R version 3.3.2 (R Core Team 2016).

Results

Chronologies

Annually resolved tree-ring width (TRW) chronologies based on a minimum of 10 cross-sections were obtained for the different sampling sites (Figure S2). Average ring width was 51.68 µm (SD=16.72), with a maximum measured value of 304.10 µm at Sørkapp. Average correlations between cross-section chronologies within plants were high (rbar.wt=[0.58:0.72]). While the average correlations between plant chronologies within sites were relatively low (rbar.bt= [0.17:0.36]) (i.e. a relatively high between-plant variation), the Expressed Population Signal were still high (EPS=[0.69:0.87]).

Local analysis

Model selection of full models containing the same set of variables for each site revealed differences in the slope of relationship between RWI and covariates between sites. All climate variables proposed in the full model were able to explain some portion of growth, as the top-ranking models (ΔAICc<2) contained all of the variables in one combination or another across sites (Table S2).

The most parsimonious models (Table 2) revealed a positive effect of July temperature on growth in three out of four sites (Figure 2). A strong negative effect of ROS on growth was detected in the two west-coast sites closest to the ocean (ca. 200-250 m distance), Ny-Ålesund and Kapp Linné. Snow accumulation had a slightly positive effect on growth at Ny-Ålesund, and was among the top-ranking models at three out of four sites. Precipitation in July was included in the most parsimonious model at Kapp Linné, but the effect was small. There was a strong negative delayed growth response in two out of four sites.

Regional analysis

Table 3 shows the results from the selected model on the regional scale with the estimated regional variables, allowing for differential growth response among sites, as well as the results from a more general "Svalbard" model (see Table S3 for models with ΔAICc<2). In the model exploring the among-site variations, the effect of regional estimates of July temperature on growth was positive, and did not vary among sites (additive effect). In addition, regional estimates of ROS as well as growth at time *t*-1 were selected as interaction terms with site in the best model. The strong negative effect of ROS was detected in the same sites as in the local analysis. The strength (and sign) of the delayed growth response differed among sites. The yearly variance in RWI explained 6.4% of the total random variation (number of groups (i.e. years) =36).

In the overall "Svalbard" model, the regional estimate of July temperature and growth at time *t*-1 were selected in the best model. In the "Svalbard" model, year (number of groups= 36) explained 6.0% of

the random variance in RWI. On the regional scale, the regional estimate of July temperature and the general Svalbard *S. polaris* chronology are correlated to a high degree (r=0.56, P<.001, n=34) (Figure 3).

Because *S. polaris* RWI did not show any consistent responses to the detrended large-scale climate proxies in neither of the models, the analyses are not presented.

Synchrony analysis

Shrub growth showed significant spatial synchrony across large distances: the average regional synchrony was 0.23 (95% CI: [0.11:0.39]) and the spatial scale of synchrony was estimated to be 192 km (Figure 4a). Weather data from all stations (Table S1) were highly synchronized over large scales, with for instance an average regional synchrony of 0.55 (95% CI: [0.14:0.89]) and a spatial scale of synchrony estimated to 342 km for July temperature. From the regional analysis, the regional estimate of July temperature was considered the main potentially synchronizing climate variable. Average regional synchrony in model residuals when accounting for the effect of July temperature remained significant, but was reduced to 0.17 (95% CI: [0.03:0.32]). The spatial scale of synchrony was estimated to 153 km (Figure 4b). The mean difference in average regional synchrony before and after accounting for July temperature was 0.09 (95% CI= [0.01:0.19]) (Figure 5).

Maximum likelihood (ML) estimates of yearly average regional synchrony revealed a significant decrease in synchrony over time (β= -0.02, SE=±.006, P=<.001), i.e. a decrease in avarage regional synchrony of 0.2 for every 10 years (Figure 6). The average regional synchrony was reduced to almost zero in the five most recent years.

Yearly ML estimates of synchrony in the detrended key climate variables did not show any clear changes over time (β =-.006, SE=±.009, P=0.53 for July temperature and β= .004, SE=±.007, P=0.64 for ROS). However, examining the changes in synchrony over time in non-detrended climate variables revealed a significant decrease in the levels of synchrony in July temperature over time (β= -.006, SE=±.002, P=.003), while there was no clear change in non-detrended ROS (β= 0.07, SE=±.006, P=0.22) (Figure S4). Directly comparing the relation between the decreased levels of synchrony observed in the non-detrended climate variables to the pattern found in the detrended growth data (RWI) may be difficult. Therefore, I perform a separate analysis of this relationship using raw, non-detrended ring width measurements (TRW). The decreasing pattern of ML estimates of yearly average regional synchrony in TRW was similar to the pattern observed in the standardized RWI data (β= -.005, SE=±.002, P=0.01), and I found a significant positive relationship between the observed changes in synchrony in TRW and in July temperature (linear regression: β= 0.39, SE=±.17, P=0.03) (Figure 7).

Discussion

By applying dendrochronological tools on the dwarf shrub *S. polaris*, this study has demonstrated how climate fluctuations synchronize plant growth over large distances across Svalbard, a high-Arctic hotspot for climate change. While heavy winter rain-on-snow (ROS) events appear to negatively impact growth, yet only in some wet coastal sites, summer temperature has an overall strong positive effect on tree-ring growth (Figure 2 and 3) and, hence, explains a significant part of the spatial synchrony in plant growth (Figure 4 and 5). However, the growth synchrony shows a marked decline since the late 1990s (Figure 6), possibly as a result of the reduced spatial synchrony in summer climate (Figure 7) occurring in parallel with the recent warming trend.

The Moran effect predicts that environmental variables can synchronize population fluctuations over large areas (Moran, 1953). Climate-growth analysis of arctic dwarf-shrub chronologies from numerous single sites across the Arctic demonstrate the large influence that climatic variables, and in particular, summer temperature, have on plant growth (Bär et al. 2008, Schmidt et al. 2010, Blok et al. 2011, Rayback et al. 2012a, Buchwal et al. 2013, Franklin 2013, Beil et al. 2015, Myers-Smith et al. 2015a). However, large-scale studies examining growth synchrony and the role of climatic drivers to such patterns in the Arctic have been lacking so far, probably because obtaining growth chronologies from dwarf-shrubs is difficult and time-consuming (due to extremely narrow growth rings and numerous morphological challenges), and because of low accessibility to many places at high latitudes. Thus, the chronologies developed in this study represent a valuable contribution to our understanding of spatiotemporal patterns in past primary production, and hence ecosystem dynamics in the Arctic, one of the places on Earth most sensitive to climate change (IPPC 2014). Further, the unique long-term weather station data that exists on Svalbard has a remarkably high spatial resolution for such a northerly location, providing a rare opportunity to quantify the climatic contribution to the observed synchrony.

Comparing these large-scale, long-term data sets, I found clear evidence that summer temperature contributes considerably to shaping primary production. Locally, this key climatic variable was detected as the main driver of ring-width fluctuations at (almost) all sites. Importantly, I found that summer temperature contributes to the synchronization of primary production across large distances in this ecosystem. To my knowledge, this is the first study demonstrating the role of climate in synchronizing Arctic plant growth at a large spatial scale. Such quantification of the role of climatic factors in shaping ecosystem dynamics is important for our ability to understand and predict the broader ecological impacts of climate change to take appropriate management and conservation decisions. While extinction risk is probably not particularly relevant for a highly abundant shrub species

like *S. polaris*, its observed climate-induced tree-ring growth fluctuations likely reflects overall primary production patterns operating across large spatiotemporal scales (Le Moullec et al. in prep.). This implies that more vulnerable species than S. *polaris* may be impacted more dramatically by changes in the (climate) variables driving growth synchronization.

The Arctic is changing, and is predicted to become increasingly warmer (especially during winter) and wetter (Rennert et al. 2009, IPCC 2014, Brönnimann 2015). Extreme weather events such as ROS are observed to increase (and predicted to increase further) in frequency in many parts of the Arctic (Bokhorst et al. 2008, Rennert et al. 2009, Hansen et al. 2014). A strong negative effect of ROS-events on primary production was found at the relatively warm and humid west-coastal sites in close proximity to the ocean, and these sites are likely to represent future conditions across Svalbard and the Arctic in general. Ecosystem implications of ROS-events have only recently received attention, but dramatic consequences of ROS-events on Arctic herbivore populations (by blocking access to primary production) have been reported (Kohler and Aanes 2004, Rennert et al. 2009, Hansen et al. 2014). The consequences of ROS for primary production are not well understood, but Milner et al (2016) found that ROS had negative effects on shoot survival and flowering in the Arctic shrub *Cassiope tetragona*, while promoting growth in surviving shoots. The findings from this study should be considered an additional early warning sign, with an urgent need for further in-depth investigations across species and over large spatial scales.

Temporal fluctuations in growth synchrony can occur in relation to climatic variation (Läänelaid et al. 2012), and hence the observed decrease of average regional synchrony over time may be related to the recent climate-related changes occurring in Svalbard (Nordli et al. 2014). These findings indicate an increasing heterogeneity in growth fluctuations among sites. A qualitatively similar reduction in synchrony was detected in summer temperature (i.e. the main predictor of *S. polaris* growth) in recent years, indicating that low spatial synchrony in summer temperature reduces plant growth synchrony. The mechanism behind the observed decrease in plant growth synchrony are likely complex involving changes in trophic interactions due to e.g. trends in herbivore abundances, as well as other abiotic factors. For instance, there is not enough high-resolution weather data available to reliably estimate spatiotemporal patterns in ROS (or precipitation patterns in general), a weather phenomenon which has increased in frequency (Hansen et al. 2014) yet with different effects on growth among sites. Furthermore, the decrease in synchrony occurs in parallel with a major change in sea-ice extent, which is likely to influence large-scale productivity patterns (Bhatt et al. 2010). However, I found no strong evidence for large-scale impacts of regional sea-ice extent (or the Arctic Oscillation, a regional weather proxy; Aanes et al. 2002, Stenseth et al. 2003) on *S. polaris* growth patterns.

The results of this work provide novel and important insight into how spatiotemporal climate patterns, including climate change, influence terrestrial primary production in the high Arctic. The chronologies that were developed are robust due to extensive serial sectioning with four radial measurements per cross-section and cross-dating at multiple levels. Despite the trade-off I faced between number of individual chronologies constructed at each site and the number of sites for which an average chronology was constructed, statistical quality-check of the chronologies (accounting for number of individuals) revealed EPS values similar to those frequently reported for dwarf-shrub chronologies (e.g. Forbes et al. 2010, Blok et al. 2011, Rayback et al. 2012b, Buchwal et al. 2013). However, the Arctic is a harsh environment, and each individual chronology reflects the wide array of abiotic and biotic disturbances that each plant had to cope with throughout its life (Billings 1987, Crawford 1997), thus causing high between-plant variation. Therefore, at the local scale, increasing the sample size would likely reveal even stronger effects of the key climatic drivers and contribute to clarify the role of other climate variables, such as snow accumulation or summer precipitation, which also showed tendencies to influence growth. The negative delayed growth response found in most sites may be a result of trade-offs between growth and allocating resources to e.g. damage repair in response to perturbations, or reproduction. The strength of such trade-offs can vary among sites, depending on the harshness of the local environment, but further studies are needed to investigate these relations.

At the regional scale, the synchrony in plant growth is possibly underestimated, as correlation estimates are highly sensitive to the high between-plant variation. Accordingly, the difference between observed plant growth synchrony and that of the key climatic driver, i.e. summer temperature, is likely amplified. Despite these challenges, a synchronizing effect of summer temperature was detectable over large distances, a relation that would emerge even clearer with increasing sample size (i.e. number of sites and/or number of plants). In addition, linear detrending of both growth and climate variables was performed in this study to avoid reporting spurious correlations due to common but unrelated trends. This conservative approach increases the confidence with which the results from this work can be reported, but has likely reduced the strength of the climate-growth relationships.

As expected, a relatively high proportion of the observed synchrony remained unexplained after accounting for the effect of summer temperature. This is likely due to the observed synchrony being a combination of different climatic variables affecting growth simultaneously. Also the effect of summer temperature on synchrony was evaluated only for July. The growing season differs in length and onset among sites, and in e.g. the warm valley of Semmeldalen, primary production has also been found to be influenced by temperatures in June (Van der Wal and Stien 2014, Le Moullec et al. in prep.). Further, the contribution of trophic interactions to the observed synchrony in growth has not been evaluated here. While a meta-study by Bernes et al. (2013) on *R. tarandus* grazing impact on Arctic and Alpine

vegetation in general conclude that grazing has only little impact on woody plants in these ecosystems, little is known about the grazing impact of herbivores on *S. polaris* (but see Gillespie et al. 2013).

In conclusion, the work presented here thus answers the research questions posed. I found that A1: while summer temperature had an overall strongly positive effect on *S. polaris* tree-ring growth across Svalbard, growth responded strongly negatively to rain-on-snow at some wet coastal sites. A2: Shrub growth on Svalbard was correlated over large distances, and summer temperature contributed significantly to the observed synchrony, and A3: there was a marked decline in the spatial synchrony in plant growth since the late 1990s, which could be partly explained by the reduced spatial synchrony in summer temperatures occurring in parallel with the overall warming trend. These findings may have fundamental implications for understanding Arctic ecosystems in space and time.

Acknowledgements

This project was financed by the Research Council of Norway (POLARPROG project 216051, Centre of Excellence project 223257, KLIMAFORSK project 244647, Arctic Field Grant project 246054) and Svalbard Environmental Protection Fund (project 16/113).

I profoundly want to thank all of my supervisors for giving me the opportunity that this thesis has proven to be, for your endless patience with me, and the many hours (and hundreds of mails) of great discussions and feedback. Thank you, Mathilde, for never giving up on this project, for your dedication and hard work, and for your friendship. Thank you, Brage and Vidar for your invaluable guidance and expertise, and for your massive moral support.

Great appreciation goes to Agata Buchwal for teaching us the science of dendrochronology, applied to one of the most difficult shrubs on Earth. Thanks to you Mathilde, Marlène, and René for the great time we spent together in the field, that was a once-in-a-lifetime experience. I would like to express my gratitude to the expedition team on board the *Sillage*, Morgan Lizabeth Bender, Christophe and Marie-Diane Vanquathem and Mathilde, for making it possible to access the most remote places of the Arctic, and for your tremendous efforts (involving bleeding and freezing fingers) to bring back home the most beautiful shrubs. I would like to thank the Norwegian Polar Institute, and in particular, Åshild Ønvik Pedersen for her contribution to the fieldwork logistics. I thank the Institute of Geophysics Polish Academy of Sciences and meteorological staff of the Polish Polar Station Hornsund for delivering air temperature and precipitation data. Thanks to Torbjørn Østby for providing the downscaled ERA-Interim data for us. Thank you, Bart for helping me with structuring the meteorological data. A big thank you to Dora Marie Alvsvåg, Tone Kjersti Kåsi and Sigrid Lindmo for your great help and company during lab-work and digitalizing.

I want to thank my family and friends for all your support and encouragement, and for always being there for me.

References

Aanes, R., B. E. Sæther, F. M. Smith, E. J. Cooper, P. A. Wookey, and N. A. Øritsland. 2002. The Arctic Oscillation predicts effects of climate change in two trophic levels in a high-arctic ecosystem. Ecology Letters **5**:445-453.

Aerts, R., J. Cornelissen, and E. Dorrepaal. 2006. Plant performance in a warmer world: general responses of plants from cold, northern biomes and the importance of winter and spring events. Plant Ecology **182**:65-77.

Barbour, M. H., J. H. Burk, and W. D. Pitts. 1980. Terrestrial plant ecology. Benjamin Cummings, Menlow Park, California, U.S.A.

Bartoń, K. 2013. MuMIn: multi-model inference. R package version 1.9.13

Beil, I., A. Buras, M. Hallinger, M. Smiljanić, and M. Wilmking. 2015. Shrubs tracing sea surface temperature—Calluna vulgaris on the Faroe Islands. International journal of biometeorology **59**:1567-1575.

Bernes, C., K. A. Bråthen, B. C. Forbes, A. Hofgaard, J. Moen, and J. D. Speed. 2013. What are the impacts of reindeer/caribou (*Rangifer tarandus L.*) on arctic and alpine vegetation? A systematic review protocol. Environmental Evidence **4**:1-26.

Bhatt, U. S., D. A. Walker, M. K. Raynolds, J. C. Comiso, H. E. Epstein, G. Jia, R. Gens, J. E. Pinzon, C. J. Tucker, and C. E. Tweedie. 2010. Circumpolar Arctic tundra vegetation change is linked to sea ice decline. Earth Interactions **14**:1-20.

Billings, W. 1987. Constraints to plant growth, reproduction, and establishment in arctic environments. Arctic and Alpine Research **16:**357-365.

Biondi, F., and F. Qeadan. 2008. A theory-driven approach to tree-ring standardization: defining the biological trend from expected basal area increment. Tree-Ring Research **64**:81-96.

Bjørkvoll, E., B. Pedersen, H. Hytteborn, I. S. Jónsdóttir, and R. Langvatn. 2009. Seasonal and interannual dietary variation during winter in female Svalbard reindeer (*Rangifer tarandus platyrhynchus*). Arctic, Antarctic, and Alpine Research **41**:88-96.

Bjørnstad. 2016. ncf: Spatial Nonparametric Covariance Functions. R package version 1.1–7. 2016.

Bjørnstad, F., Wilhelm, and N. C. Stenseth. 1995. A Geographic Gradient in Small Rodent Density Fluctuations: A Statistical Modelling Approach. Proceedings of the Royal Society of London, Series B **262**:127-133.

Bjørnstad, O. N., R. A. Ims, and X. Lambin. 1999. Spatial population dynamics: analyzing patterns and processes of population synchrony. Trends in Ecology & Evolution **14**:427-432.

Blok, D., U. Sass-Klaassen, G. Schaepman-Strub, M. Heijmans, P. Sauren, and F. Berendse. 2011. What are the main climate drivers for shrub growth in Northeastern Siberian tundra? Biogeosciences **8**:1169-1179.

Bokhorst, S., J. Bjerke, F. Bowles, J. Melillo, T. Callaghan, and G. Phoenix. 2008. Impacts of extreme winter warming in the sub-Arctic: growing season responses of dwarf shrub heathland. Global Change Biology **14**:2603-2612.

Bowman, D. M., R. J. Brienen, E. Gloor, O. L. Phillips, and L. D. Prior. 2013. Detecting trends in tree growth: not so simple. Trends in plant science **18**:11-17.

Briffa, K. R., and T. M. Melvin. 2011. A closer look at regional curve standardization of tree-ring records: justification of the need, a warning of some pitfalls, and suggested improvements in its application. Pages 113-145 *in* M. K. Hughes, T. W. Swetnam, and H. F. Diaz, editors. Dendroclimatology. Springer, Dordrecht, Netherlands.

Brown, M. 2015. AutoStitch [Computer Program].

Brönnimann, S. 2015. Climatic Changes Since 1700. Springer, Cham, Swizerland.

Buchwal, A. 2014. Constraints on dendrochronological dating of *Salix polaris* from central Spitsbergen. Czech Polar Reports **4**:73 - 79.

Buchwal, A., G. Rachlewicz, P. Fonti, P. Cherubini, and H. Gartner. 2013. Temperature modulates intra-plant growth of *Salix polaris* from a high Arctic site (Svalbard). Polar Biology **36**:1305-1318.

Bunn, A. G. 2008. A dendrochronology program library in R (dplR). Dendrochronologia **26**:115-124.

Buras, A., M. Hallinger, and M. Wilmking. 2012. Can shrubs help to reconstruct historical glacier retreats? Environmental Research Letters **7**:1-8.

Buras, A., and M. Wilmking. 2014. Straight lines or eccentric eggs? A comparison of radial and spatial ring width measurements and its implications for climate transfer functions. Dendrochronologia **32**:313-326.

Burnham, K. P., and D. R. Anderson. 2002. Model selection and multimodel inference: a practical information-theoretic approach. 3d edition. Springer, New York, U.S.A.

Büntgen, U., and F. H. Schweingruber. 2010. Environmental change without climate change? New Phytologist **188**:646-651.

Bär, A., A. Bräuning, and J. Löffler. 2006. Dendroecology of dwarf shrubs in the high mountains of Norway – A methodological approach. Dendrochronologia **24**:17-27.

Bär, A., A. Bräuning, and J. Löffler. 2007. Ring-width chronologies of the alpine dwarf shrub Empetrum hermaphroditum from the Norwegian mountains. Iawa Journal **28**:325-338.

Bär, A., R. Pape, A. Bräuning, and J. Löffler. 2008. Growth-ring variations of dwarf shrubs reflect regional climate signals in alpine environments rather than topoclimatic differences. Journal of Biogeography **35**:625-636.

Cook, E., and N. Pederson. 2011. Uncertainty, Emergence, and Statistics in Dendrochronology. Pages 77-112 *in* M. K. Hughes, T. W. Swetnam, and H. F. Diaz, editors. Dendroclimatology: progress and prospects, developments in paleoecological research. Springer, Berlin, Germany.

Crawford, R. M. 1997. Habitat fragility as an aid to long-term survival in arctic vegetation. Pages 113-137 *in* S. J. Woodin and M. Marquiss, editors. Ecology of Arctic Environments: 13th Special Symposium of the British Ecological Society. Blackwell Science Ltd. Oxford, England

Eberhart-Phillips, L. J., B. R. Hudgens, and M. A. Colwell. 2016. Spatial synchrony of a threatened shorebird: Regional roles of climate, dispersal and management. Bird Conservation International **26**:119-135.

Engen, S., R. Lande, and B. E. Sæther. 2002. The spatial scale of population fluctuations and quasi-extinction risk. The American Naturalist **160**:439-451.

Engen, S., R. Lande, B. E. Sæther, and T. Bregnballe. 2005. Estimating the pattern of synchrony in fluctuating populations. Journal of Animal Ecology **74**:601-611.

Engen, S., and B.-E. Sæther. 2005. Generalizations of the Moran effect explaining spatial synchrony in population fluctuations. The American Naturalist **166**:603-612.

Estay, S. A., A. A. Albornoz, M. Lima, M. S. Boyce, and N. C. Stenseth. 2011. A simultaneous test of synchrony causal factors in muskrat and mink fur returns at different scales across Canada. PloS one **6**:1-8.

Forbes, B. C., M. Fauria, and P. Zetterberg. 2010. Russian Arctic warming and 'greening'are closely tracked by tundra shrub willows. Global Change Biology **16**:1542-1554.

Franklin, R. S. 2013. Growth response of the alpine shrub, Linanthus pungens, to snowpack and temperature at a rock glacier site in the eastern Sierra Nevada of California, USA. Quaternary International **310**:20-33.

Gers, E., N. Florin, H. Gartner, T. Glade, R. Dikau, and F. H. Schweingruber. 2001. Application of shrubs for dendrogeomorphological analysis to reconstruct spatial and temporal landslide movement patterns-A preliminary study. Zeitschrift für Geomorphologie. Supplementband:163-175.

Gillespie, M. A. K., I. S. Jónsdóttir, I. D. Hodkinson, and E. J. Cooper. 2013. Aphid–willow interactions in a high Arctic ecosystem: responses to raised temperature and goose disturbance. Global Change Biology **19**:3698-3708.

Gornall, J., S. Woodin, I. Jónsdóttir, and R. van der Wal. 2011. Balancing positive and negative plant interactions: how mosses structure vascular plant communities. Oecologia **166**:769-782.
Grøtan, V., B.-E. Sæther, S. Engen, E. J. Solberg, J. D. Linnell, R. Andersen, H. Brøseth, and E. Lund. 2005. Climate causes large-scale spatial synchrony in population fluctuations of a temperate herbivore. Ecology **86**:1472-1482.
Gärtner, H., S. Lucchinetti, and F. H. Schweingruber. 2014. New perspectives for wood anatomical analysis in dendrosciences: the GSL1-microtome. Dendrochronologia **32**:47-51.
Hallinger, M., M. Manthey, and M. Wilmking. 2010. Establishing a missing link: warm summers and winter snow cover promote shrub expansion into alpine tundra in Scandinavia. New Phytologist **186**:890-899.
Hallinger, M., and M. Wilmking. 2011. No change without a cause–why climate change remains the most plausible reason for shrub growth dynamics in Scandinavia. New Phytologist **189**:902-908.
Hansen, B. B., V. Grøtan, R. Aanes, B.-E. Sæther, A. Stien, E. Fuglei, R. A. Ims, N. G. Yoccoz, and Å. Ø. Pedersen. 2013. Climate events synchronize the dynamics of a resident vertebrate community in the high Arctic. Science **339**:313-315.
Hansen, B. B., K. Isaksen, R. E. Benestad, J. Kohler, Å. Ø. Pedersen, L. E. Loe, S. J. Coulson, J. O. Larsen, and Ø. Varpe. 2014. Warmer and wetter winters: characteristics and implications of an extreme weather event in the High Arctic. Environmental Research Letters **9**:114021.
Heino, M., V. Kaitala, E. Ranta, and J. Lindström. 1997. Synchronous dynamics and rates of extinction in spatially structured populations. Proceedings of the Royal Society of London, Series B **264**:481-486.
Henry, G., and U. Molau. 1997. Tundra plants and climate change: the International Tundra Experiment (ITEX). Global Change Biology **3**:1-9.
Hisdal, V. 1985. Geography of Svalbard. 2nd edition. Norsk Polarinstitutt, Tromsø, Norway
Hohenstein, S., and R. Kliegl. 2015. remef: Remove partial effects. R package version 1.0. 6.9000.
Ims, R., D. Ehrich, B. Forbes, B. Huntley, D. Walker, P. Wookey, D. Berteaux, U. Bhatt, K. Bråthen, and M. Edwards. 2013. Terrestrial ecosystems. Pages 384-441 *in* Arctic Biodiversity Assessment. Status and trends in Arctic biodiversity. Conservation of Arctic Flora and Fauna (CAFF), Akureyri, Iceland.
Ims, R. A., and H. P. Andreassen. 2000. Spatial synchronization of vole population dynamics by predatory birds. Nature **408**:194-196.
Ims, R. A., and E. Fuglei. 2005. Trophic interaction cycles in tundra ecosystems and the impact of climate change. BioScience **55**:311-322.
IPCC. 2014. Climate change 2014: synthesis Report. Contribution of working groups I, II and III to the fifth assessment report of the intergovernmental panel on climate change. [Core Writing Team, R.K. Pachauri and L.A. Meyer (eds.)]. IPCC, Geneva, Switzerland.
Johansen, B. E., S. R. Karlsen, and H. Tømmervik. 2012. Vegetation mapping of Svalbard utilising Landsat TM/ETM+ data. Polar Record **48**:47-63.
Jonasson, S., and T. V. Callaghan. 1992. Root mechanical properties related to disturbed and stressed habitats in the Arctic. New Phytologist **122**:179-186.
Koenig, W. D. 1999. Spatial autocorrelation of ecological phenomena. Trends in Ecology & Evolution **14**:22-26.
Koenig, W. D., and J. M. Knops. 2013. Large-scale spatial synchrony and cross-synchrony in acorn production by two California oaks. Ecology **94**:83-93.
Kohler, J., and R. Aanes. 2004. Effect of winter snow and ground-icing on a Svalbard reindeer population: results of a simple snowpack model. Arctic, Antarctic, and Alpine Research **36**:333-341.
Kolishchuk, V. 1990. Dendroclimatological study of prostrate woody plants. Pages 51–55 *in* Cook E*,* Kairiukstis L*,* editors*.* Methods of dendrochronology: applications in the environmental sciences*.* Kluwer Academic Publishers, London, England.

Lande, R., S. Engen, and B.-E. Sæther. 1999. Spatial scale of population synchrony: environmental correlation versus dispersal and density regulation. The American Naturalist **154**:271-281.
LeBlanc, D. C. 1990. Relationships between breast-height and whole-stem growth indices for red spruce on Whiteface Mountain, New York. Canadian Journal of Forest Research **20**:1399-1407.
Liebhold, A., W. D. Koenig, and O. N. Bjørnstad. 2004. Spatial synchrony in population dynamics. Annual review of ecology, evolution, and systematics **35**:467-490.
Läänelaid, A., S. Helama, A. Kull, M. Timonen, and J. Jaagus. 2012. Common growth signal and spatial synchrony of the chronologies of tree-rings from pines in the Baltic Sea region over the last nine centuries. Dendrochronologia **30**:147-155.
Massie, T. M., G. Weithoff, N. Kuckländer, U. Gaedke, and B. Blasius. 2015. Enhanced Moran effect by spatial variation in environmental autocorrelation. Nature Communications **6**:1-8.
Milner, J. M., Ø. Varpe, R. Wal, and B. B. Hansen. 2016. Experimental icing affects growth, mortality, and flowering in a high Arctic dwarf shrub. Ecology and evolution. **6:** 2139-2148.
Moran, P. A. P. 1953. The statistical analysis of the Canadian lynx cycle. II. Synchronization and meteorology. Aust. J. Zool. **1**:291-298.
Myers-Smith, I. H., S. C. Elmendorf, P. S. A. Beck, M. Wilmking, M. Hallinger, D. Blok, K. D. Tape, S. A. Rayback, M. Macias-Fauria, B. C. Forbes, J. D. M. Speed, N. Boulanger-Lapointe, C. Rixen, E. Levesque, N. M. Schmidt, C. Baittinger, A. J. Trant, L. Hermanutz, L. S. Collier, M. A. Dawes, T. C. Lantz, S. Weijers, R. H. Jorgensen, A. Buchwal, A. Buras, A. T. Naito, V. Ravolainen, G. Schaepman-Strub, J. A. Wheeler, S. Wipf, K. C. Guay, D. S. Hik, and M. Vellend. 2015a. Climate sensitivity of shrub growth across the tundra biome. Nature Clim. Change **5**:887-891.
Myers-Smith, I. H., M. Hallinger, D. Blok, U. Sass-Klaassen, S. A. Rayback, S. Weijers, A. J. Trant, K. D. Tape, A. T. Naito, S. Wipf, C. Rixen, M. A. Dawes, J. A. Wheeler, A. Buchwal, C. Baittinger, M. Macias-Fauria, B. C. Forbes, E. Lévesque, N. Boulanger-Lapointe, I. Beil, V. Ravolainen, and M. Wilmking. 2015b. Methods for measuring arctic and alpine shrub growth: A review. Earth-Science Reviews **140**:1-13.
Nieminen, M. 2015. Distance decay is uncommon in large-scale population synchrony of common moths: does it promote vulnerability to climate change? Insect Conservation and Diversity **8**:438-447.
Nordli, Ø., R. Przybylak, A. E. Ogilvie, and K. Isaksen. 2014. Long-term temperature trends and variability on Spitsbergen: the extended Svalbard Airport temperature series, 1898-2012. Polar Research **33**.1-23.
Oksanen, T., L. Oksanen, J. Dahlgren, and J. Olofsson. 2008. Arctic lemmings, *Lemmus spp*. and Dicrostonyx spp.: integrating ecological and evolutionary perspectives. Evolutionary Ecology Research **10**:415-434.
Owczarek, P. 2010. Dendrochronological dating of geomorphic processes in the High Arctic. Landform Analysis **14**:45-56.
Polunin, N. 1955. Attempted dendrochronological dating of ice island T-3. Science **122**:1184-1186.
Post, E. 2003. Large-scale climate synchronizes the timing of flowering by multiple species. Ecology **84**:277-281.
Post, E., and M. C. Forchhammer. 2002. Synchronization of animal population dynamics by large-scale climate. Nature **420**:168-171.
Post, E., M. C. Forchhammer, M. S. Bret-Harte, T. V. Callaghan, T. R. Christensen, B. Elberling, A. D. Fox, O. Gilg, D. S. Hik, T. T. Høye, R. A. Ims, E. Jeppesen, D. R. Klein, J. Madsen, A. D. McGuire, S. Rysgaard, D. E. Schindler, I. Stirling, M. P. Tamstorf, N. J. C. Tyler, R. van der Wal, J. Welker, P. A. Wookey, N. M. Schmidt, and P. Aastrup. 2009. Ecological Dynamics Across the Arctic Associated with Recent Climate Change. Science **325**:1355-1358.
Power, M. E. 1992. Top-down and bottom-up forces in food webs: do plants have primacy. Ecology **73**:733-746.
Preece, C., and G. Phoenix. 2014. Impact of early and late winter icing events on sub-arctic dwarf shrubs. Plant Biology **16**:125-132.

R Core Team (2016) R: A language and environment for statistical computing. R Foundation for Statistical Computing, Vienna, Austria.
Ranta, E., V. Kaitala, J. Lindstrom, and H. Linden. 1995. Synchrony in population dynamics. Proceedings of the Royal Society of London, Series B **262**:113-118.
Rathgeber, C. B., H. E. Cuny, and P. Fonti. 2016. Biological basis of tree-ring formation: a crash course. Frontiers in Plant Science **7**:1-7.
Rayback, S. A., G. H. Henry, and A. Lini. 2012a. Multiproxy reconstructions of climate for three sites in the Canadian High Arctic using Cassiope tetragona. Climatic Change **114**:593-619.
Rayback, S. A., and G. H. R. Henry. 2005. Dendrochronological Potential of the Arctic Dwarf-Shrub Cassiope tetragona. Tree-Ring Research **61**:43-53.
Rayback, S. A., A. Lini, and D. L. Berg. 2012b. The dendroclimatological potential of an alpine shrub, Cassiope mertensiana, from Mount Rainier, WA, USA. Geografiska Annaler: Series A, Physical Geography **94**:413-427.
Rennert, K. J., G. Roe, J. Putkonen, and C. M. Bitz. 2009. Soil thermal and ecological impacts of rain on snow events in the circumpolar Arctic. Journal of Climate **22**:2302-2315.
Rosenstock, T. S., A. Hastings, W. D. Koenig, D. J. Lyles, and P. H. Brown. 2011. Testing Moran's theorem in an agroecosystem. Oikos **120**:1434-1440.
Royama, T. 1992. Analytical population dynamics. Chapman&Hall, London, England.
Rønning, O. I. 1996. The flora of Svalbard. 3d edition. Norsk Polarinstitutt, Oslo, Norway.
Sakshaug E, G. H. Johnsen, S. Kristiansen, C. von Quillfeldt, F. Rey, D. Slagstad, F. Thingstad. 2009. Phytoplankton and primary production. Pages 167-208 *in* Ecosystem Barents Sea. E. Sakshaug, G. Johnsen, K. Kovacs, editors. Tapir Academic Press, Trondheim, Norway.
Schindelin, J., C. T. Rueden, M. C. Hiner, and K. W. Eliceiri. 2015. The ImageJ ecosystem: an open platform for biomedical image analysis. Molecular reproduction and development **82**:518-529.
Schmidt, N. M., C. Baittinger, and M. C. Forchhammer. 2006. Reconstructing century-long snow regimes using estimates of high arctic Salix arctica radial growth. Arctic, Antarctic, and Alpine Research **38**:257-262.
Schmidt, N. M., C. Baittinger, J. Kollmann, and M. C. Forchhammer. 2010. Consistent dendrochronological response of the dioecious *Salix arctica* to variation in local snow precipitation across gender and vegetation types. Arctic, Antarctic, and Alpine Research **42**:471-475.
Schweingruber, F. H., and P. Poschlod. 2005. Growth rings in herbs and shrubs: life span, age determination and stem anatomy. Forest Snow and Landscape Research **79**: 195-415.
Semenchuk, P. R., B. Elberling, and E. J. Cooper. 2013. Snow cover and extreme winter warming events control flower abundance of some, but not all species in high arctic Svalbard. Ecology and evolution **3**:2586-2599.
Sheppard, L. W., J. R. Bell, R. Harrington, and D. C. Reuman. 2015. Changes in large-scale climate alter spatial synchrony of aphid pests. Nature Climate Change. **6**:610-613.
Speed, J. D., G. Austrheim, A. J. Hester, and A. Mysterud. 2011. Browsing interacts with climate to determine tree-ring increment. Functional Ecology **25**:1018-1023.
Stenseth, N. C. 1999. Common dynamic structure of Canada lynx populations within three climatic regions. Science **285**:1071-1073.
Stenseth, N. C., G. Ottersen, J. W. Hurrell, A. Mysterud, M. Lima, K. S. Chan, N. G. Yoccoz, and B. Ådlandsvik. 2003. Studying climate effects on ecology through the use of climate indices: the North Atlantic Oscillation, El Nino Southern Oscillation and beyond. Proceedings of the Royal Society of London B: Biological Sciences **270**:2087-2096.
Sæther, B.-E., S. Engen, A. P. Møller, E. Matthysen, F. Adriaensen, W. Fiedler, A. Leivits, M. M. Lambrechts, M. E. Visser, T. Anker-Nilssen, C. Both, A. A. Dhondt, R. H. McCleery, J. McMeeking, J. Potti, O. W. Røstad, and D. Thomson. 2003. Climate variation and regional gradients in population dynamics of two hole-nesting passerines. Proceedings of the Royal Society B: Biological Sciences **270**:2397-2404.

Sæther, B. E., S. Engen, V. Grøtan, W. Fiedler, E. Matthysen, M. E. Visser, J. Wright, A. P. Møller, F. Adriaensen, and H. Van Balen. 2007. The extended Moran effect and large-scale synchronous fluctuations in the size of great tit and blue tit populations. Journal of Animal Ecology **76**:315-325.

Tardif, J. C., and F. Conciatori. 2015. Microscopic examination of wood: Sample preparation and techniques for light microscopy. Pages 373-415 *in* Plant Microtechniques and Protocols. E. C. T. Yeunges, C. Stasolla, M. J. Sumner and B. Q. Huang, editors. Springer, Swizerland.

van der Wal, R., N. Madan, S. Van Lieshout, C. Dormann, R. Langvatn, and S. Albon. 2000. Trading forage quality for quantity? Plant phenology and patch choice by Svalbard reindeer. Oecologia **123**:108-115.

van der Wal, R., and A. Stien. 2014. High-arctic plants like it hot: a long-term investigation of between-year variability in plant biomass. Ecology **95**:3414-3427.

Vazquez-Cooz, I., and R. W. Meyer. 2002. A differential staining method to identify lignified and unlignified tissues. Biotechnic & Histochemistry **77**:277-282.

Visser, H. 1995. Note on the relation between ring widths and basal area increments. Forest science **41**:297-304.

Wahren, C. H., M. Walker, and M. Bret-Harte. 2005. Vegetation responses in Alaskan arctic tundra after 8 years of a summer warming and winter snow manipulation experiment. Global Change Biology **11**:537-552.

Wigley, T. M., K. R. Briffa, and P. D. Jones. 1984. On the average value of correlated time series, with applications in dendroclimatology and hydrometeorology. Journal of climate and Applied Meteorology **23**:201-213.

Wipf, S., V. Stoeckli, and P. Bebi. 2009. Winter climate change in alpine tundra: plant responses to changes in snow depth and snowmelt timing. Climatic Change **94**:105-121.

Woodcock, H., and R. S. Bradley. 1994. *Salix arctica* (Pall.): its potential for dendroclimatological studies in the High Arctic. Dendrochronologia **12**:11-22.

Woodward, F. I. 1987. Climate and plant distribution. Cambridge University Press, Cambridge, England.

Ydenberg, R. C. 1987. Nomadic predators and geographical synchrony in microtine population cycles. Oikos **50**:270-272.

Østby, T. I., T. V. Schuler, J. O. Hagen, R. Hock, J. Kohler, and C. H. Reijmer. 2017. Diagnosing the decline in climatic mass balance of glaciers in Svalbard over 1957–2014. The Cryosphere **11**:191-215.

Tables

Table 1. Sampling site description and *S. polaris* tree-ring width (TRW) chronology statistics. Vegetation type is presented in accordance with Johansen et al. (2012) using a 1 km buffer area. Average annual and July ERA-temperature (°C) and averagle annual total ERA-precipitation (mm) are estimated from ERA-Interim downscaled to 1 km (Østby et al. 2017). The chronologies contain a minimum of 10 cross sections for the given time-span. Total number of plants, cross-sections and radii measured are given, as well as the standard descriptive statistics within- and between-plant interseries correlation (rbar.wt and rbar.bt) as well as Expressed Population Signal (EPS).

	Ny-Ålesund	**Petuniabukta**[b]	**Kapp Linné**	**Semmeldalen**[c]	**Hornsund**	**Sørkapp**	**Diskobukta**	**Vossebukta**
Coordinates (Lat./Lon.)	78°93 N, 11°92 E	78°43 N, 16°37° E	78°00 N, 13°67 E	77°90 N, 15°20 E	77°00 N, 15°55 E	76°48 N, 16°56 E	77°93 N, 21°46° E	78°45 N, 20°48 E
Vegetation type[a]	Exposed Dryas tundra	Exposed Dryas tundra	Established Dryas tundra	Arctic meadow	Established Dryas tundra	Gravel snowbed	Exposed Dryas tundra	Exposed Dryas tundra
ERA annual temp. (°C)	-5.4	-7.7	-3.4	-6.1	-3.4	-2.1	-5.5	-6.2
ERA July temp. (°C)	3.9	3.5	4.9	4.6	4.2	4.6	3.0	3.2
ERA annual precip. (mm)	655	450	635	589	897	680	518	577
Chronology time-span	1986-2014	1942-2010	1977-2014	1986-2014	1962-2014	1989-2014	1976-2014	1974-2014
Total plants	5	10	5	27	5	5	5	5
Total sections	24	142	27	139	23	25	28	25
(Total radii)	(96)	(471)	(108)	(556)	(92)	(100)	(112)	(100)
rbar.wt	0.65	*NA*	0.64	0.65	0.72	0.60	0.68	0.58
rbar.bt	0.32	0.40	0.22	0.17	0.32	0.31	0.36	0.32
EPS	0.80	0.87	0.69	0.86	0.77	0.82	0.82	0.81

a: Johansen et al (2012), b: Buchwal et al (2013), c: Le Moullec et al, in prep.

Table 2. Coefficient estimates (β), standard error (SE) and test statistics (t- and P-values) of the most parsimonious model for the local analysis of *Salix polaris* RWI at each sampling site where detailed local weather data was available. Growth and covariates are detrended for the maximal overlapping time-span for each site. Residual variance (Var) and number of groups (N) are given for the random effects on intercept. Growth(*t*-1)= growth in year *t*-1; July temperature= Average July temperature (°C); July precipitation= Total July precipitation (mm); ROS = ln-transformed total precipitation (mm) falling as rain (>0°C) November through April; Snow = Total precipitation (mm) falling as snow (<0°C) November through April.

Local analysis								
	Ny-Ålesund		**Kapp Linné**		**Hornsund**		**Semmeldalen[a]**	
Fixed effects	**β±SE**	**t (P)**	**β±SE**	**t (P)**	**β±SE**	**t (P)**	**β±SE**	**t (P)**
Intercept	0.03 ±0.12	0.23 (0.82)	-0.04 ±0.08	-0.48 (0.64)	0.02 ±0.11	0.16 (0.88)	.003 ±0.04	0.08 (0.94)
Growth(*t*-1)	-0.32 ±0.09	-3.76 (<.001)	-	-	-0.12 ±0.07	-1.59 (0.11)	-0.12 ±0.04	-2.68 (0.01)
July temperature	-	-	0.38 ±0.13	3.03 (0.01)	0.44 ±0.19	2.32 (0.03)	0.22 ± 0.06	3.67 (<.001)
July precipitation	-	-	.006 ±.004	1.54 (0.14)	-	-	-	-
ROS	-0.26 ±0.08	-3.11 (0.01)	-0.32 ±0.07	-4.43 (<.001)	-	-	-	-
Snow	.003 ±.002	1.87 (0.08)	-	-	-	-	-	-
Random effects	**Var**	**N**	**Var**	**N**	**Var**	**N**	**Var**	**N**
Year	0.22	26	0.03	20	0.28	35	0.03	27

a: Le Moullec et al (in prep.)

Table 3. Coefficient estimates (β), Standard error (SE) and test statistics (t- and P-values) of the most parsimonious model for the regional analysis of *Salix polaris* RWI exploring among-site heterogeneities, as well as for a "Svalbard" model, excluding site as fixed effect. Growth and covariates are detrended for the maximal overlapping time-span for each site. Growth(*t*-1)= growth in year *t*-1; July temperature= estimated regional July temperature (°C); ROS = ln-transformed estimated regional total precipitation (mm) falling as rain (>0°C) November through April. Note that July temperature is selected as an additive effect in the model investigating differences among sites, so that estimates do not differ among sites. Estimates and standard error are given in 10^{-2}.

Regional analysis																		
	«Svalbard»		**Ny-Ålesund**		**Petuniabukta**		**Kapp Linné**		**Hornsund**		**Semmeldalen**		**Sørkapp**		**Diskobukta**		**Vossebukta**	
Fixed effects	**β±SE**	**t (P)**	**β±SE**	**t (P)**	**β±SE**	**t (P)**	**β±SE**	**t (P)**	**β±SE**	**t (P)**	**β±SE**	**t (P)**	**β±SE**	**t (P)**	**β±SE**	**t (P)**	**β±SE**	**t (P)**
Intercept	-1.42 ±3.56	-0.40 (0.69)	-2.17 ±8.45	-0.26 (0.80)	-3.54 ±6.94	-0.51 (0.61)	-6.34 ±7.77	-0.08 (0.94)	0.32 ±7.79	0.04 (0.97)	-2.29 ±6.44	-0.36 (0.72)	-3.00 ±8.66	-0.35 (0.73)	-6.10 ±7.79	-0.08 (0.94)	0.35 ±6.41	0.06 (0.96)
July temperature	25.08 ±6.71	3.74 (>.001)	24.27 ±6.90	3.52 (.001)	24.27 ±6.90	3.52 (.001)	24.27 ±6.90	3.52 (.001)	24.27 ±6.90	3.52 (.001)	24.27 ±6.90	3.52 (.001)	24.27 ±6.90	3.52 (.001)	24.27 ±6.90	3.52 (.001)	24.27 ±6.90	3.52 (.001)
ROS	-	-	-28.04 ±8.65	-3.24 (.001)	-8.60 ±6.70	-1.28 (0.20)	-18.02 ±7.66	-2.35 (0.02)	1.11 ±7.48	0.15 (0.88)	-8.76 ±6.70	-1.31 (0.19)	-1.87 ±9.43	-0.20 (.0.84)	-10.94 ±7.63	-1.43 (0.15)	6.54 ±6.19	1.01 (0.29)
Growth(*t*-1)	-17.36 ±2.34	-7.43 (>.001)	-17.85 ±8.90	-2.01 (0.05)	15.14 ±9.89	1.53 (0.13)	15.42 ±8.68	1.78 (0.08)	-2.30 ±8.21	-0.28 (0.78)	7.55 ±8.31	0.90 (0.36)	-21.14 ±10.20	-2.10 (0.04)	32.98 ±9.93	3.32 (>.001)	-20.02 ±6.28	-3.19 (.001)

Figure legends

Figure 1. Vegetation map of Svalbard (Johansen et al. 2012) where sampling localities (filled red circles) and weather stations (black stars) are shown. Spot diameter represents sampling effort (5-30) per site.

Figure 2. Partial residual plots of the main climatic drivers of *Salix polaris* RWI that were detected in the local analysis. Individual chronologies and covariates, i.e. July temperature and rain-on-snow (ROS), are detrended for the maximum overlapping time-span at each site.

Figure 3. Correlation between the estimated "Svalbard" RWI- chronology and detrended estimates of yearly regional July temperature. Both time-series are presented with corresponding standard errors, and their correlation coefficient *r* is indicated.

Figure 4. Pairwise correlations (ρ) between RWI chronologies for all sites, and the spatial non-parametric correlation functions (Sncf, thick black- lines) with 95% confidence envelope (thin black lines) for (a) *Salix polaris* RWI and (b) residual RWI when accounting for detrended regional estimates of July temperature. Horizontal lines show average regional synchrony (blue dashed line) and zero synchrony (black dotted line). For each site, estimated July temperature is detrended for the time-span of the growth chronology. Plot (c) shows the Sncf for the difference in the pairwise RWI correlations and residual correlation (ρ_{res}), indicating the synchronyizing effect of July temperature on growth over large distances.

Figure 5. The synchronizing effect of July temperature on *Salix polaris* RWI. (a) Frequency distribution of the bootstrap replicates (n=1000) of the average regional synchrony in *S. polaris* RWI (blue) and of the average regional synchrony in residual RWI when accounting for detrended regional estimates of July temperature (red). (b) Frequency distribution and mean (blue dashed line) of the difference in the bootstrapped replicates of average regional synchrony before and after accounting for detrended regional estimates of July temperature, with 2.5% and 97.5% percentiles (thin black lines). The black dashed line indicates the reference level of significance at 0.

Figure 6. Maximum likelihood estimates of average regional synchrony in *Salix polaris* RWI for every year during the time-period 1989-2014.

Figure 7. Relationship between maximum likelihood estimations of yearly average synchrony in both TRW (non-detrended, non-standardized growth) and non-detrended July temperature (°C).

Figure 1.

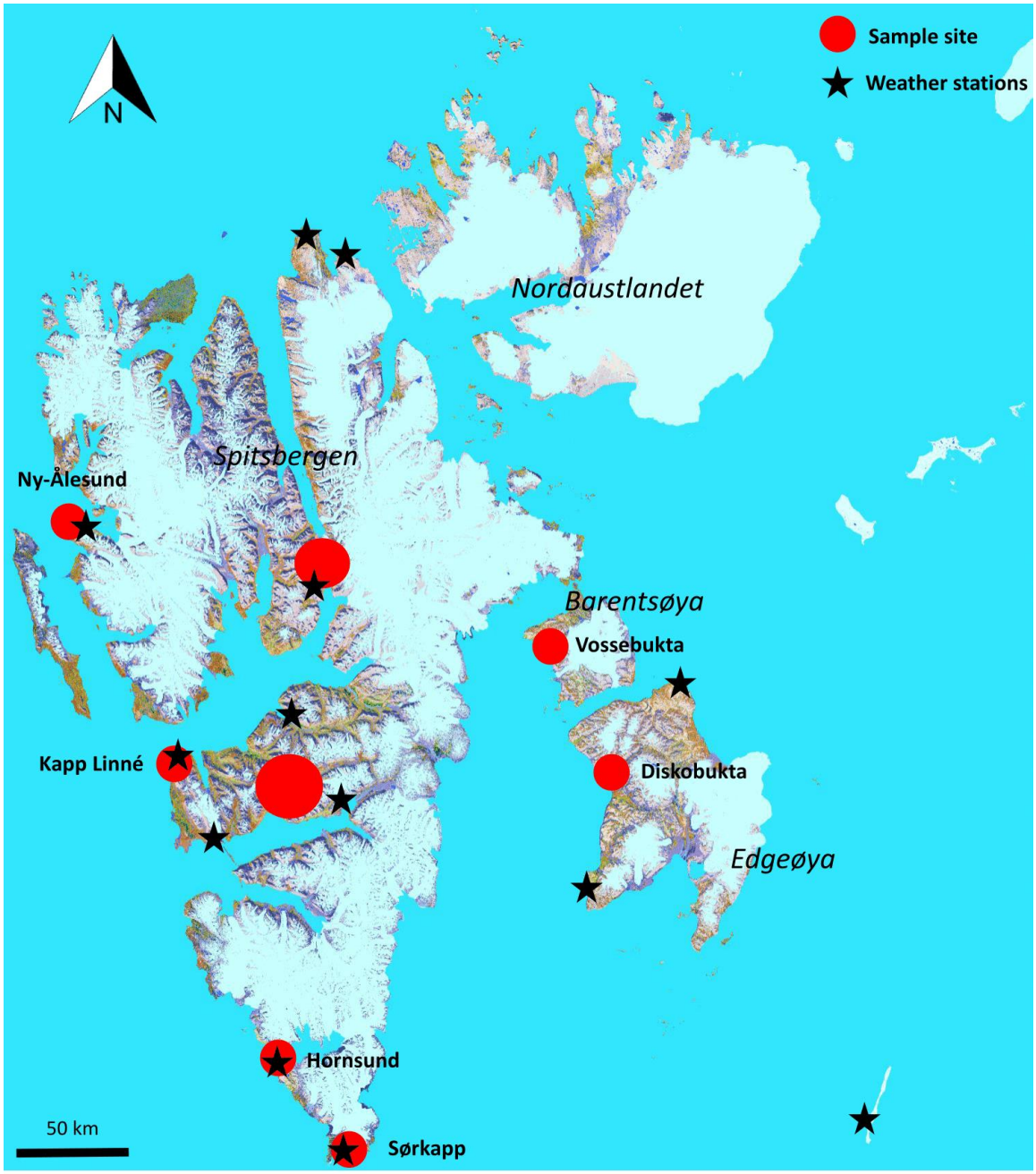
Sample site
Weather stations
N
Nordaustlandet
Spitsbergen
Ny-Ålesund
Barentsøya
Vossebukta
Kapp Linné
Diskobukta
Edgeøya
Hornsund
Sørkapp
50 km

Figure 2.

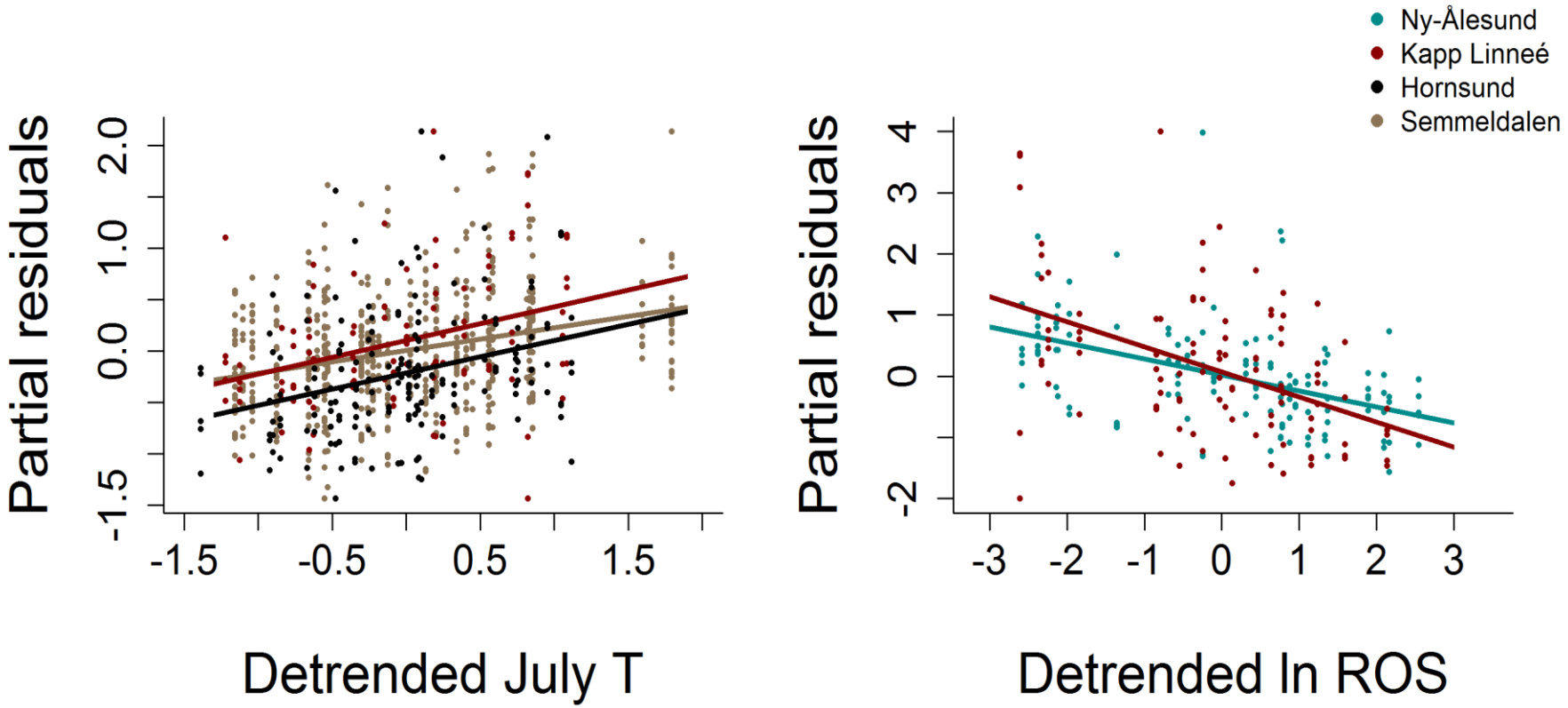
Partial residuals
-1.5
0.0
1.0
2.0
-1.5
-0.5
0.5
1.5
Detrended July T
Partial residuals
-2
0
1
2
3
4
-3
-2
-1
0
1
2
3
Detrended ln ROS
Ny-Ålesund
Kapp Linneé
Hornsund
Semmeldalen

Figure 3.

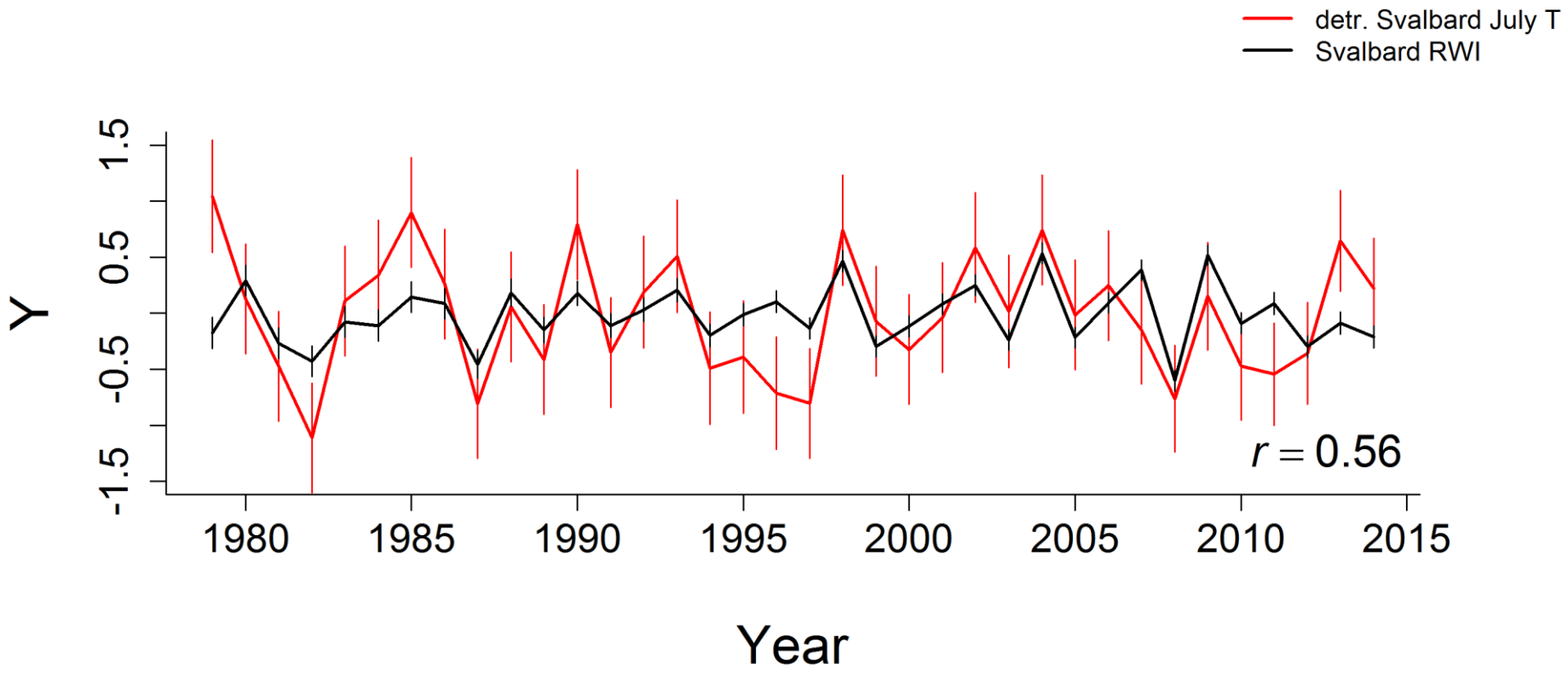
detr. Svalbard July T
Svalbard RWI
Y
1.5
0.5
-0.5
-1.5
1980
1985
1990
1995
2000
2005
2010
2015
Year
r = 0.56

Figure 4.

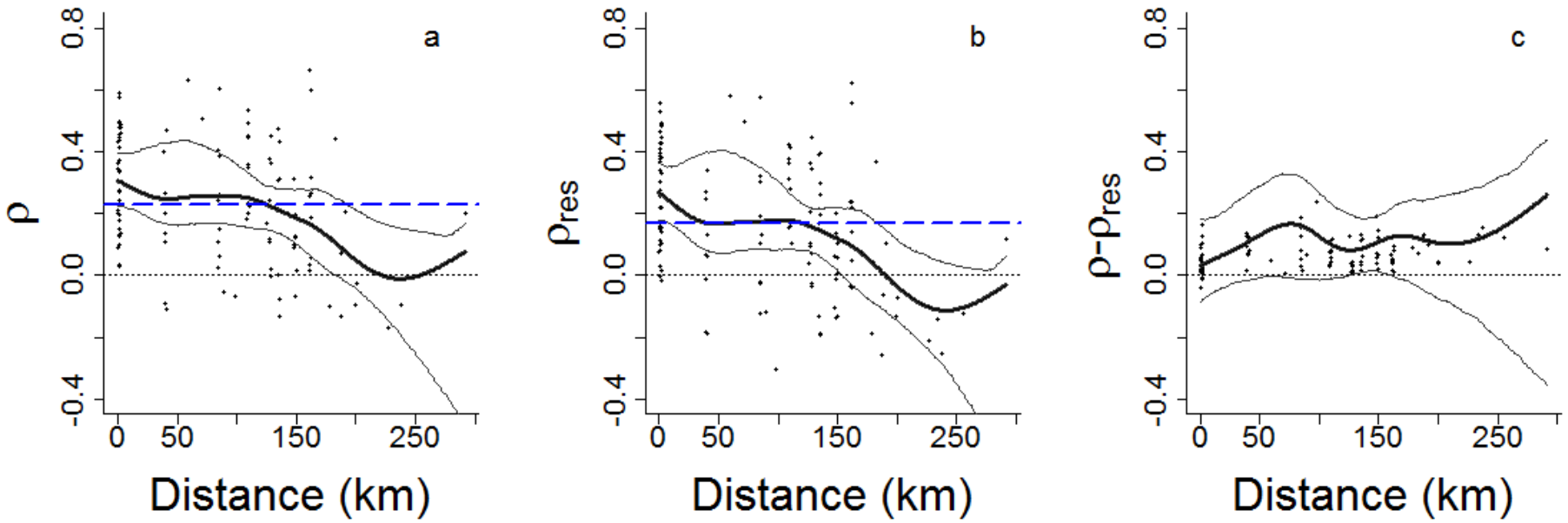

Figure 5.

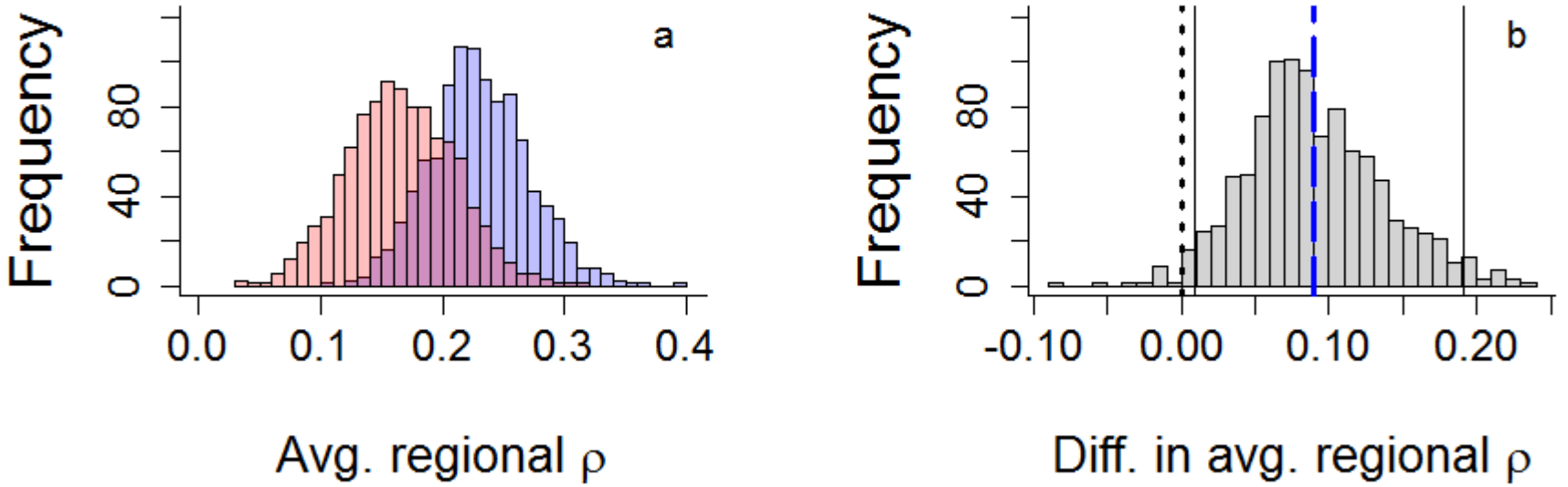
Frequency
0
40
80
a
0.0
0.1
0.2
0.3
0.4
Avg. regional ρ
Frequency
0
40
80
b
-0.10
0.00
0.10
0.20
Diff. in avg. regional ρ

Figure 6.

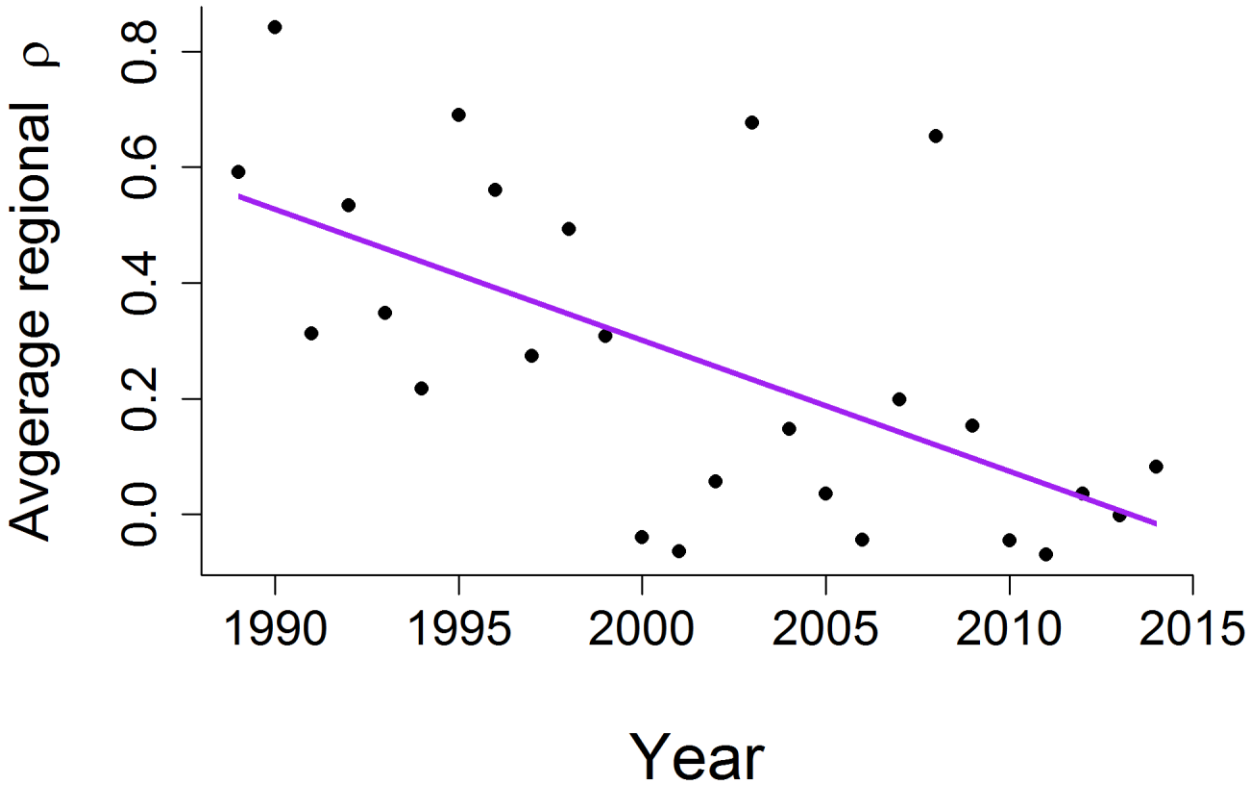
Avgerage regional ρ
0.0
0.2
0.4
0.6
0.8
1990
1995
2000
2005
2010
2015
Year

Figure 7.

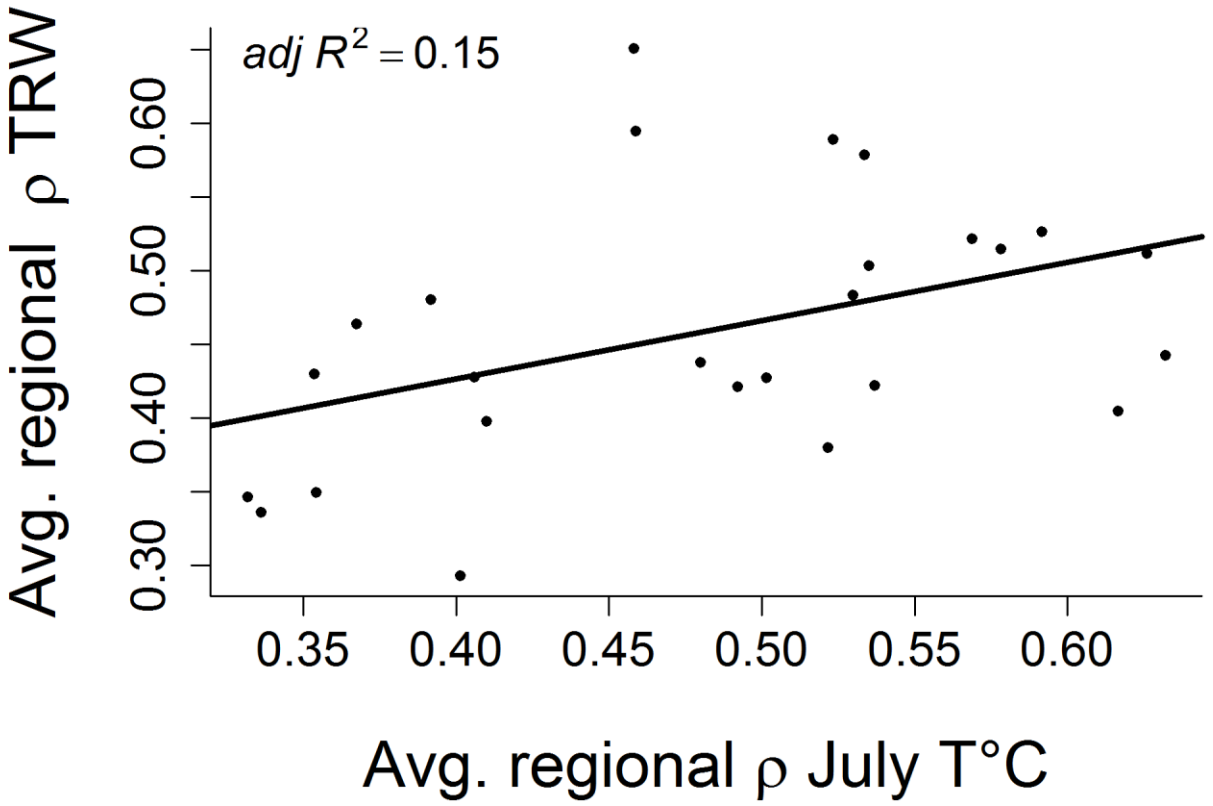
adj $R^2 = 0.15$
Avg. regional ρ TRW
0.30
0.40
0.50
0.60
0.35
0.40
0.45
0.50
0.55
0.60
Avg. regional ρ July T°C

Appendix

Weather station data

Table S1. Station name, coordinates (Lat./Lon.), time span and source of the weather station data used in this study. The data from all stations was included in the estimation of the regional climate variables. However, for the estimation of the changes in synchrony over time in weather variables, the time-series from UNIS were excluded. These time-series start only recently, and a change in number of weather stations over time can potentially bias the trend of change in synchrony.

Station	Latitude	Longitude	Time span	Source
Adventdalen_unis	78.20	15.83	2014	UNIS
Bohemanneset_unis	78.37	14.76	2014	UNIS
Breinosa_unis	78.14	16.06	2008-2010	UNIS
Jansonhaugen_unis	78.18	16.47	2011-2014	UNIS
Hornsund Station	77.00	15.54	1979-2014	Polish Polar Station Hornsund
Hopen	76.51	25.01	1947-2014	http://eklima.met.no
Edgeøya Kapp Heugelin	78.25	22.82	2007-2008 and 2011-2014	http://eklima.met.no
Svarttangen	77.53	20.83	2011-2012	http://eklima.met.no
Kongsøya	78.91	28.89	2012-2014	http://eklima.met.no
Sørkappøya	76.48	16.55	2011-2014	http://eklima.met.no
Sveagruva	77.90	16.72	1978-2014	http://eklima.met.no
Akseløya	77.69	14.78	2011-2014	http://eklima.met.no
Isfjord Radio	78.06	13.62	1947-2014	http://eklima.met.no
Barentsburg	78.05	14.23	1973-1993 and 2004-2014	www.tutiempo.net/en/Climate/BARENCBURG/07-1973/201070.htm
Svalbard Lufthavn	78.25	15.50	1975-2014	http://eklima.met.no
Longyearbyen	78.22	15.63	1957-1975	http://eklima.met.no
Pyramiden	78.66	16.36	2013-2014	http://eklima.met.no
Ny-Ålesund	78.92	11.93	1969-2014	http://eklima.met.no
Verlegenhuken	80.60	16.25	2007 and 2011-2014	http://eklima.met.no
Crozierpynten	79.92	16.84	2010-2014	http://eklima.met.no
Kvitøya	80.11	31.46	2012-2014	http://eklima.met.no
Barentsburg	78.05	14.23	1973-1993 and 2004-2014	http://eklima.met.no
Svalbard Lufthavn	78.24	15.50	1975-2014	http://eklima.met.no

Chronologies

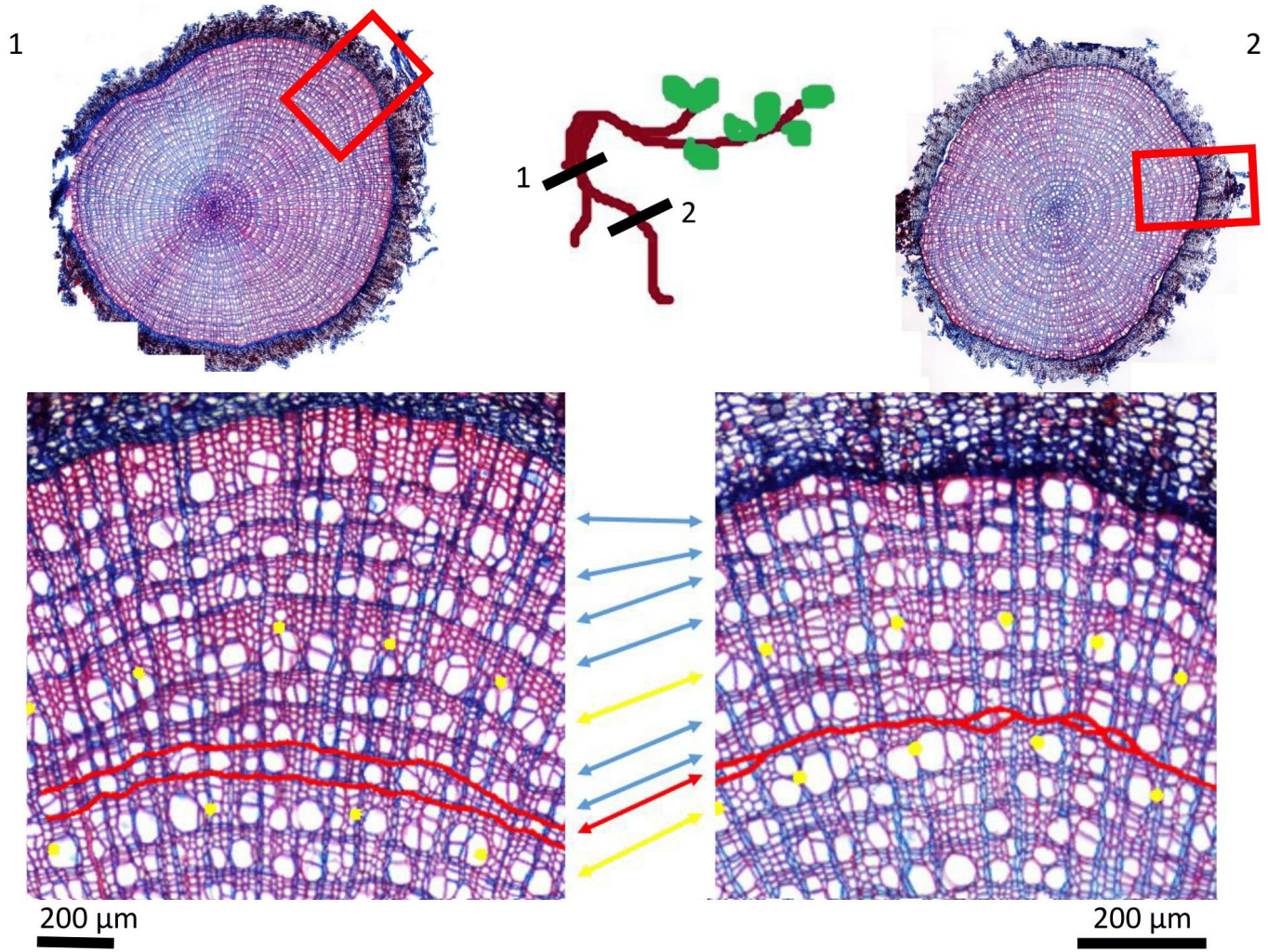

Figure S1. Illustration of the cross-dating procedure. In this example, two main-root cross-sections of an individual from Diskobukta are compared. Cross-dating by aligning pointer years (marked in yellow) makes it possible to verify the presence of a partially missing ring (PMR) in cross-section 2 (marked in red).

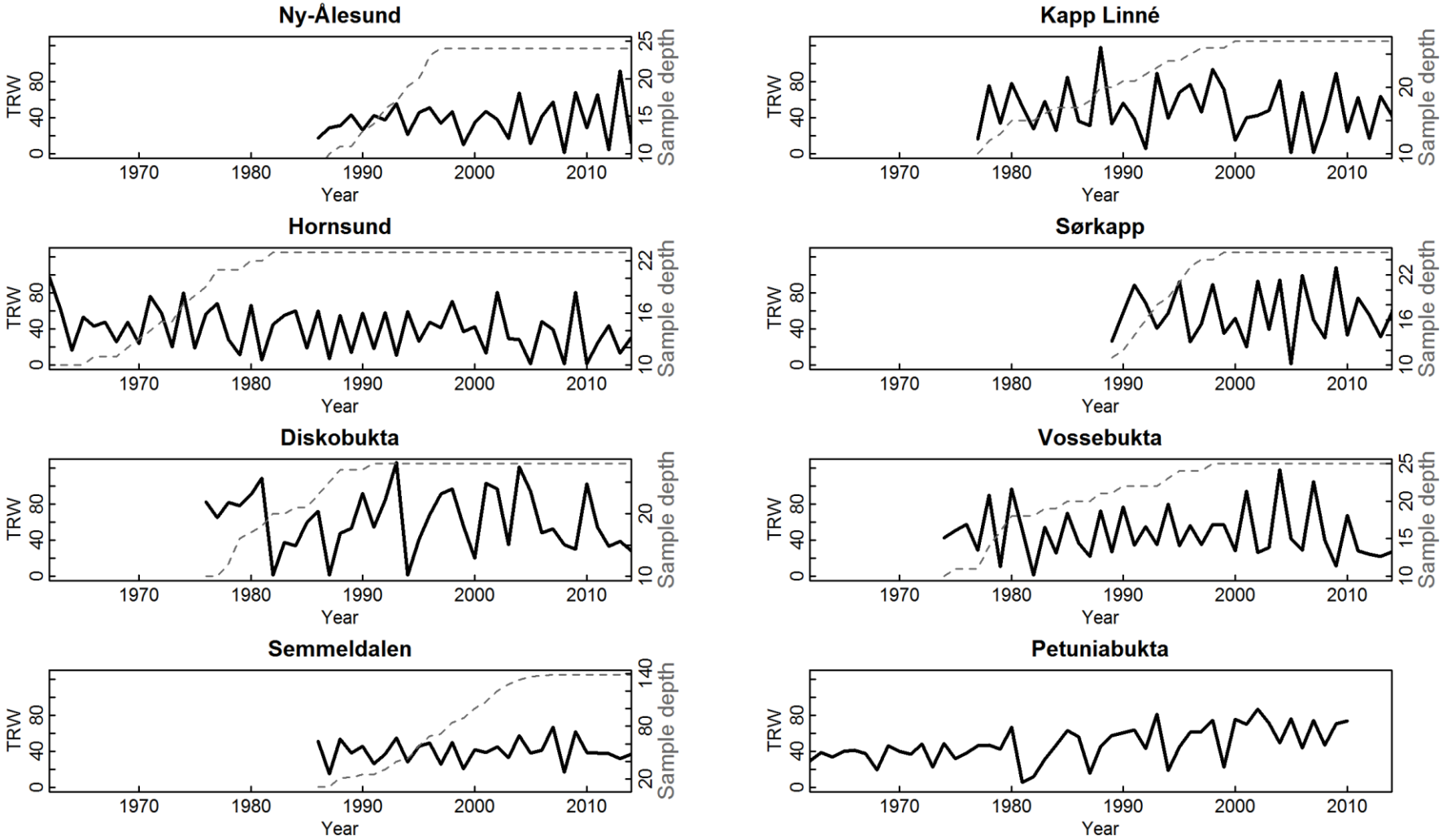

Figure S2. The *Salix polaris* TRW chronologies for the time-span at which sample depth >10 cross-sections (dashed grey line). Chronologies for Semmeldalen and Petuniabukta reported from Le Moullec et al (in prep.) and Buchwal (2013). Note that the Semmeldalen chronology contains the growth data from the nine independent sub-sites used in the synchrony analysis. The chronology for Petuniabukta is only shown for the maximum time-span for which it can be compared to the chronologies in this study, and sample depth at a yearly resolution is not available.

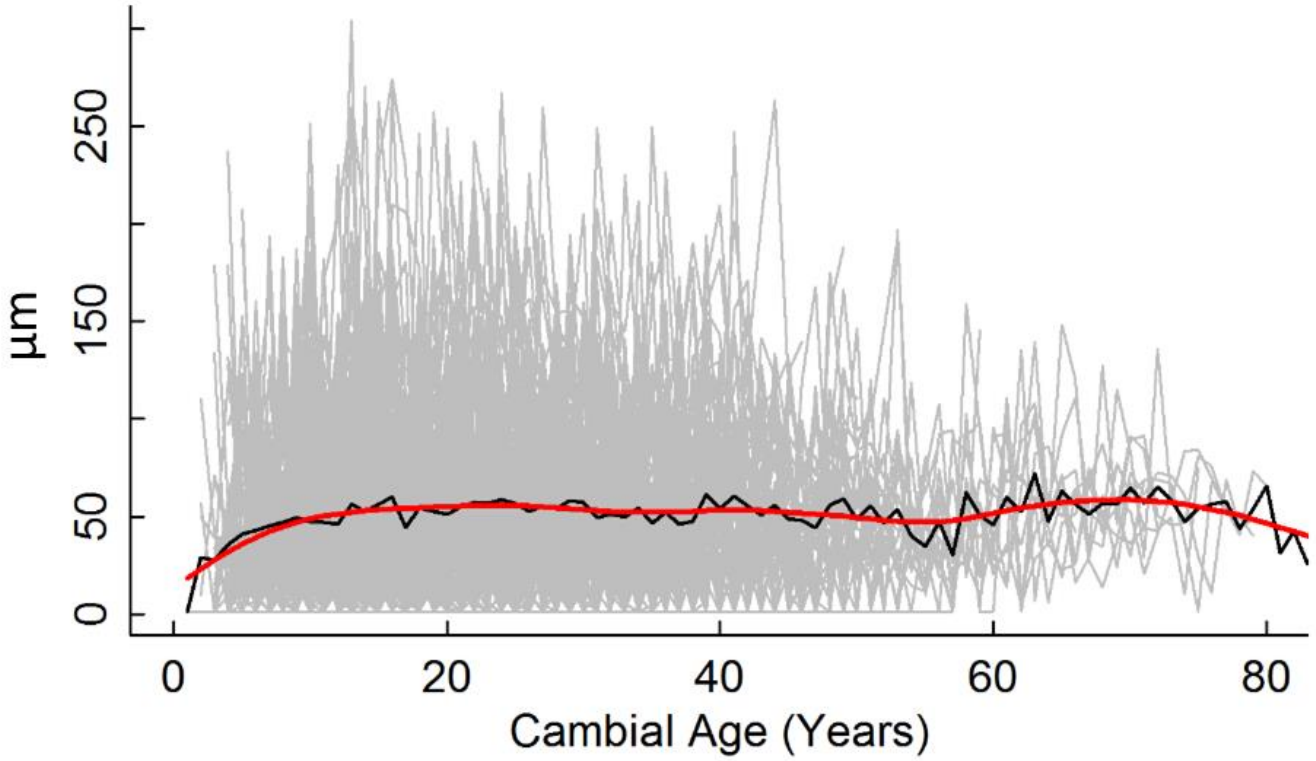

Figure S3. *Salix polaris* TRW series aligned by cambial age. The age-trend is shown as the smoothed spline (red) fitted to the mean curve (black).

Local analysis

Table S2. The top-ranking models (ΔAICc<2) for the local analysis of climatic variables on *Salix polaris* RWI. Growth and covariates are detrended for the maximal overlapping time-span for each site. Growth(*t*-1)= growth in year *t*-1; July temperature= Average July temperature (°C) ; July precipitation= Total July precipitation (mm); ROS = ln-transformed total precipitation (mm) falling as rain (>0°C) November through April; Snow= Total precipitation (mm) falling as snow (<0°C) November through April; Winter end= Julian day when the smoothed daily temperature (over 10 days) crossed 0 °C.

Site	Model	df	AICc	ΔAICc	Akaike weight
Ny-Ålesund	**Growth(*t*-1)+ ROS + Snow**	**6**	**338.33**	**0.00**	**0.36**
	Growth(*t*-1)+ ROS + Snow + July precipitation	7	338.55	0.22	0.32
	Growth(*t*-1)+ ROS	5	339.89	1.56	0.16
	Growth(*t*-1)+ ROS + July precipitation	6	339.98	1.65	0.16
Kapp Linné	**July precipitation + ROS + July temperature**	**6**	**233.33**	**0.00**	**0.46**
	ROS + July temperature	5	233.82	0.49	0.36
	July precipitation + ROS + July temperature+ Growth(t-1)	7	235.22	1.89	0.18
Hornsund	**Growth(*t*-1)+ July temperature**	**5**	**490.22**	**0.00**	**0.30**
	July temperature	4	490.66	0.44	0.24
	Growth(*t*-1)+ July temperature + Snow	6	491.94	1.72	0.13
	Growth(*t*-1)+ July temperature + Winter end	6	492.05	1.84	0.12
	Growth(*t*-1)+ July temperature + ROS	6	492.11	1.90	0.12
Semmeldalen	**Growth (*t*-1)+ July temperature**	**5**	**921.35**	**0.00**	**0.33**
	Growth (*t*-1)+ July temperature + ROS	6	921.97	0.62	0.24
	Growth (*t*-1)+ July temperature + July precipitation	6	922.53	1.18	0.18
	Growth (*t*-1)+ July temperature + ROS + July precipitation	7	923.16	1.80	0.13
	Growth (*t*-1)+ July temperature + Winter end	6	923.29	1.94	0.12

Regional analysis

Table S3. The top-ranking models (ΔAICc<2) for the regional analysis of detrended regional estimates of climate variables on *Salix polaris* RWI per site and for entire Svalbard. Growth and covariates are detrended for the maximal overlapping time-span for each site. Growth(*t*-1)= growth in year *t*-1; July temperature= Average July temperature (°C) ; July precipitation = Total July precipitation (mm); ROS = ln-transformed total precipitation (mm) falling as rain (>0°C) November through April; Snow = Total precipitation (mm) falling as snow (<0 °C) November through April; Winter end= Julian day when the smoothed daily temperature (over 10 days) crossed 0 °C.

	Model	df	AICc	Delta AICc	Akaike weight
Per site	**July temperature + ROS*site+ Growth(*t*-1)*site**	**27**	**4153.06**	**0.00**	**0.31**
	July temperature + Winter end*site+ Growth(*t*-1)*site	27	4153.57	0.51	0.24
Svalbard model	**July temperature + Growth(*t*-1)**	**5**	**4172.28**	**0.00**	**0.34**
	July temperature + Snow + Growth(*t*-1)	6	4172.78	0.50	0.26
	July temperature + ROS + Growth(*t*-1)	6	4174.12	1.84	0.13
	July temperature + Winter end+ Growth(*t*-1)	6	4174.15	1.87	0.13
	July temperature + July precipitation + Growth(*t*-1)	6	4174.18	1.90	0.13

Synchrony analysis

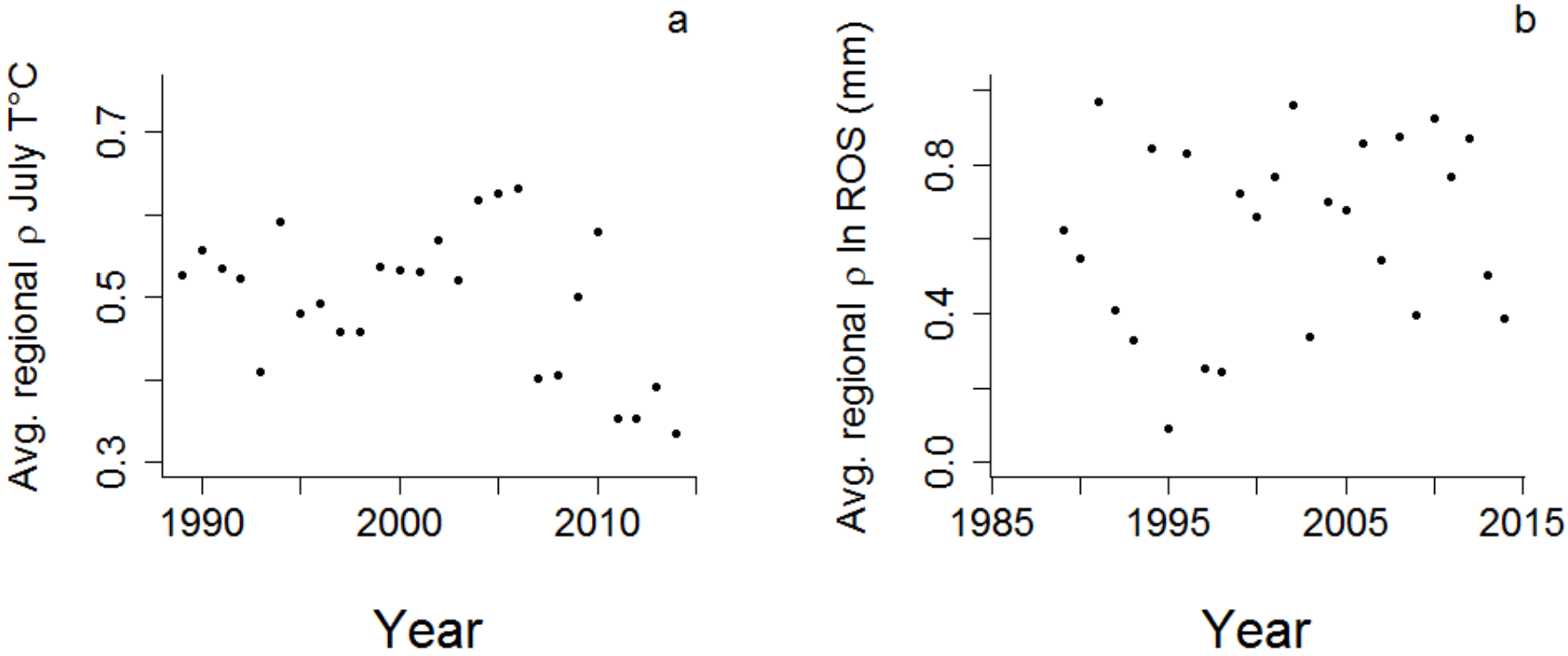

Figure S4. Estimated average regional synchrony in non-detrended (a) July temperature (°C) and (b) ln ROS (mm) during the time-period 1989-2014. Note that the scale on the y-axis is different in a) and b).